Method to design and fabricate an octahedral-tetrahedral spaceframe from repurposed scaffolding

by
Jerome Arul

B.F.A. Industrial Design, Rhode Island School of Design, 2012

Submitted to the Integrated Design and Management Program
In partial fulfillment of the requirements for the degree of

MASTER OF SCIENCE IN ENGINEERING AND MANAGEMENT

at the

MASSACHUSETTS INSTITUTE OF TECHNOLOGY

JUNE 2023

Authored by: Jerome Arul
Integrated Design and Management
May 12, 2023

Certified by: Caitlin Mueller
Associate Professor of Civil and Environmental Engineering, and Architecture
Thesis Supervisor

Accepted by: Tony Hu
Director
Integrated Design and Management Program

Method to design and fabricate an octahedral-tetrahedral spaceframe from repurposed scaffolding

by
Jerome Arul

Submitted to the Integrated Design and Management Program on May 12, 2023
In partial fulfillment of the requirements for the degree of
MASTER OF SCIENCE IN ENGINEERING AND MANAGEMENT

Abstract

Spatial structures find many applications in architecture and construction as flat trusses, but few examples take advantage of the rich variety of configurations that a multi-layered octahedral-tetrahedral (octet) spaceframe can accommodate. The octet geometry is considered because of its inherent versatility, rigidity and economy. This lattice has received renewed interest in the study of nano and microscale cellular structures due to advances in material science and additive manufacturing; we revisit the octet spaceframe in steel at the macroscale using repurposed components combined with accessible methods of fabrication.

Available connection systems for octet lattices are complex and require intensive production, and existing structural systems are proprietary or purpose-engineered solutions. This provides an opportunity to simplify the art of both joint and strut system, and document an inexpensive and open technology with broad application in resource-strapped and remote environments where material efficiency and accessible assembly are essential. This thesis demonstrates a method to design and fabricate an octet spaceframe using repurposed scaffolding.

A range of configurations and forms are modelled and generated within an octet point cloud. The structure can be evaluated in terms of human factors, utility and stiffness. The members used are commoditized steel cross-bracing with a variety of sizes that are commercially available. The joints are fabricated from steel plate using computer numerically controlled (cnc) water jet and are welded together into an orthogonal gusset. We justify a scale that is appropriate for an individual or small group to handle, fabricate and erect, with only the use of a few manual tools. A kit-of-parts of a multi-layered and multi-scale octet lattice is demonstrated, and FE methods to analyze and evaluate the structure are shown.

Thesis Supervisor: Caitlin Mueller
Title: Associate Professor of Civil and Environmental Engineering, and Architecture

Acknowledgements

I would like to express my sincere gratitude and appreciation to the following people and groups:

Professor Caitlin Mueller for enthusiastically engaging these ideas and making them coherent. Keith Lee for bringing the energy and analysis to the work, and everybody at the Digital Structures and Building Technology group. Shah Paul, Jen O'Brien, Chris Dewart, Jack Whipple, Coby Unger, and my friends at the D-Lab.

Everyone at Integrated Design and Management, Matt Kressy and Tony Hu for giving me a home at MIT. My multitalented co-instructors of nine years, Steve Eppinger and Maria Yang at Product Design and Development.

My colleagues and peers at the RISD Industrial Design department, particularly Will Reeves. Elsewhere at RISD, Mickey Ackerman for his mentorship, Stephen Metcalf for his love of geometry and Merlin Szasz for getting me started. I am grateful to the Nature Lab, particularly the Loeb Design Science Collection for all the triangles.

My parents and brother for supporting me, and my muses Erica, Maggie and Obie.

List of symbols

n – the dimension of Euclidean space
m – order of lattice through edge length division or recursion
j – joint, vertex, point, node, or connector
b – strut, edge, line, member, bar or brace
Z – number of connections per vertex
Te – tetrahedral number, number of vertices in multi-layer tetrahedron
T – triangular number, number of vertices in triangular grid
P_{cr} – Euler's critical load, at which a slender column will buckle
E – modulus of elasticity in tension or compression
q – rotational stiffness and buckling mode of column
a – cross-sectional area of column under load
l – unsupported length of column
π – ratio of circumference to diameter of a circle

Contents

1. Introduction

Methods to build and construct structures are typically in the domain of large construction entities that require significant capital, resources, and labor. There is a gap in modern construction methods for individual consumers to engage and find ownership in the process of affecting their own built environment and to find options other than traditional framing systems. Current structural systems are contingent on orthogonal frameworks, whereas the spaceframe is rich with underutilized opportunities that offer alternative means of interpreting and using space. Our built environment can be made more user-driven by incorporating principles of modularity and customization in the design process. We design and fabricate a kit of parts, using both repurposed and custom-made building components, which can be easily reassembled allowing for flexibility and adaptability in the use of space.

This research is centered on the octahedral-tetrahedral (octet) spaceframe, which is an analog of the classical truss system [1]. The geometry is also known as the *face-centered cubic* (*fcc*) or as the A_3 root lattice. The lattice is similarly-situated, meaning the connections are the same and simplifies the variety of the components in the structural system to a few types.

1.1. Octet Structures

The octet geometry is commonly used in lightweight structural applications due to its high strength-to-density ratio [2] with modern applications in architecture, novel materials, vehicles and aerospace. In architecture, trusses are known for their large spans and have the benefit of pre-fabricated components. Trusses are commonly utilized as two-layer flat systems such as roofing or facades. There are many examples of the octet used as a truss system in 20th century post war architecture [3], [4] following the increased industrial production capacity of steel and aluminum, but fewer examples of multi-layered spaceframe systems.

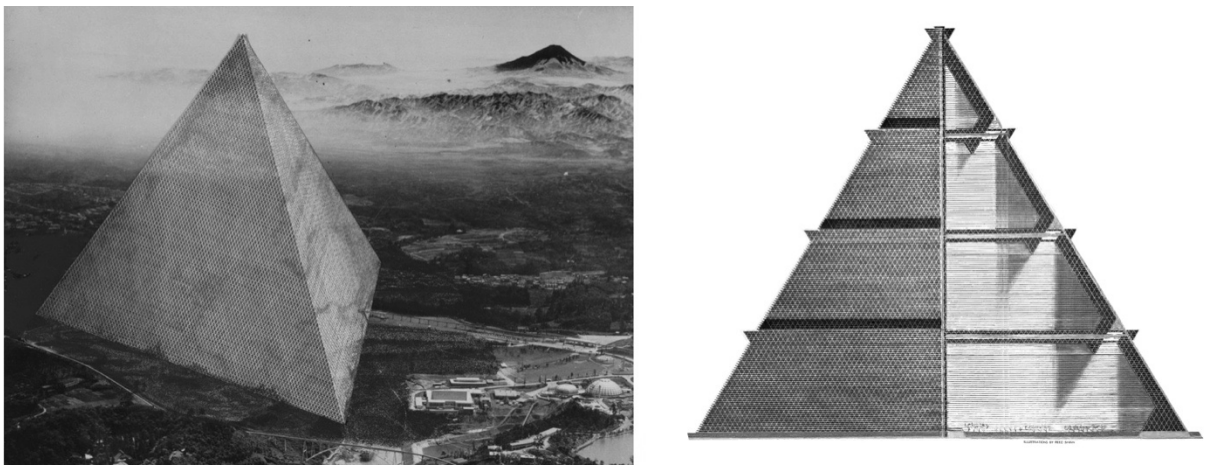

Figure 1-1: Tetrahedron City (L - R) a proposal [5] by Sadao and Fuller, 1967. Cross-section of Tetrahedron City, illustration by Reed Shinn.

Figure 1-1 shows a concept for a two-mile high tetrahedral megastructure made of octet trusses of twenty-foot modules [6] which would immerse the Japanese landscape. The proposal stretched the imagination for both economic and structural feasibility. However, the structure makes a statement about the efficiencies of modularity when applied at the industrial scale. The repetition of form and self-similarity of the components at this immense volume creates an interplay between optimal uses of space and economies of scale.

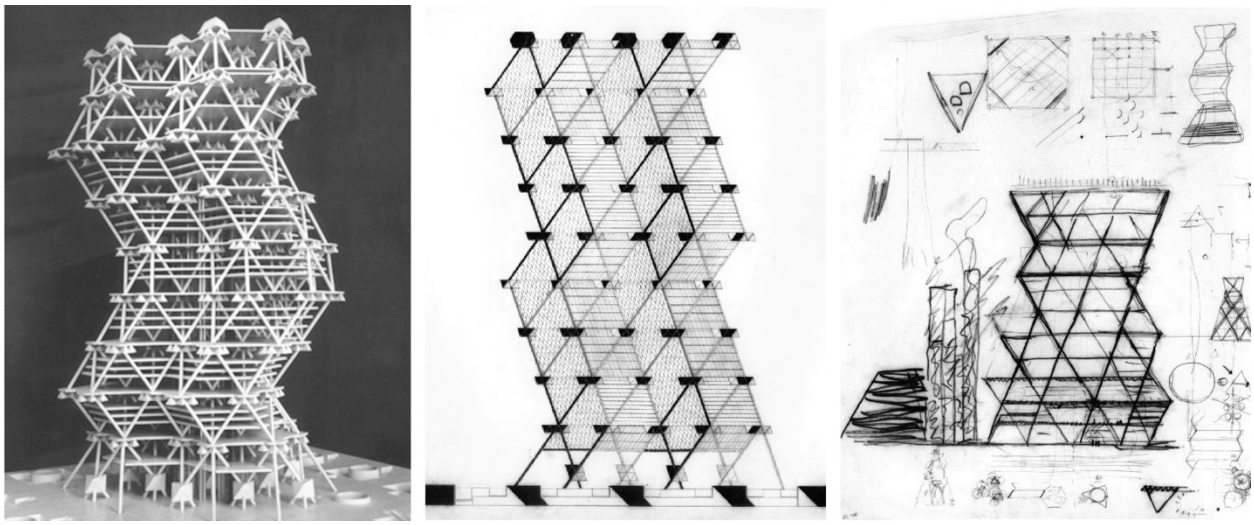

Figure 1-2: Anne Tyng Philadelphia City Tower concept (L - R) model, elevation, and rough sketches by Kahn and associates [7].

Similar to Fuller, a large body of Tyng's work was driven by an interest in fundamental geometric form. The concept for the Philadelphia City Tower stacked layers of trusses, performing slight cantilevers on all sides of the structure. The architects generated a variety of configurations through the act of drawing (figure 1-2). The members were intended to be precast and prestressed concrete with hollow sections to carry air conditioning, heating and other service lines [8]. The Gyrotron was a built example of an octet spaceframe (figure 1-3) that functioned as a fairground ride at the Expo '67. It was enclosed in a 215 ft tall [9] octahedral structure with a square floor plan, in contrast to the triangular footprints of Tyng's and Fuller's concepts. It is an early example of a structure designed with the aid of a computer. The manufacturer of the system, Alcan, used 245 tons of aluminum to fabricate the structure [10] and consisted of tubes that were 5 to 8 inches in diameter [3].

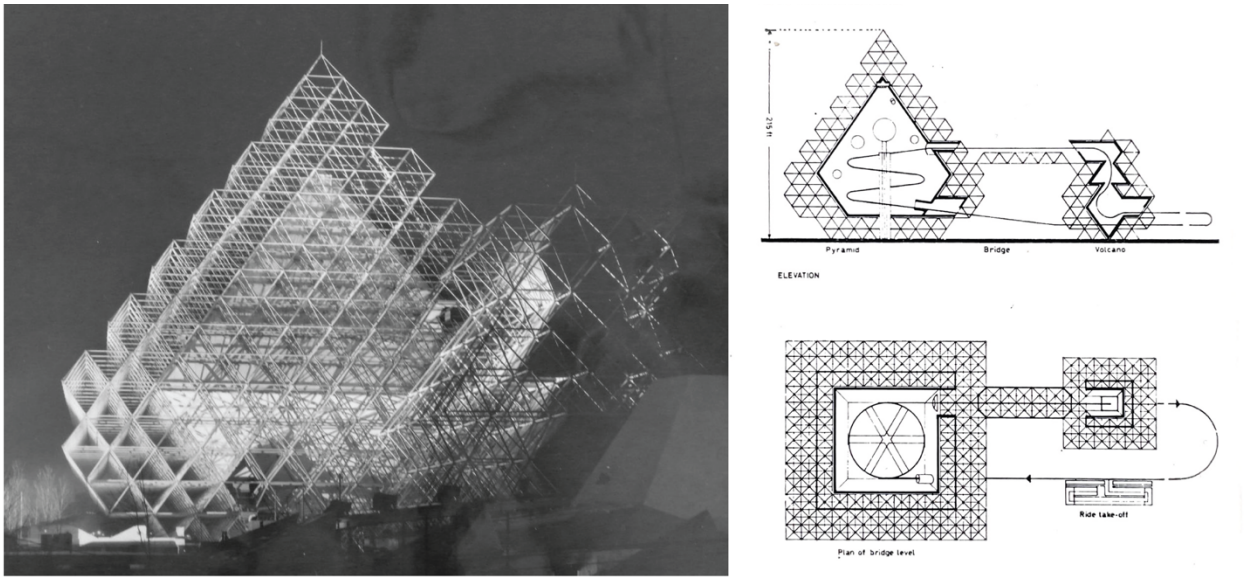

Figure 1-3: (L - R) Gyrotron at La Ronde, Expo 67, Montréal, Québec [11], Plan and elevation [9]

1.2. Connectors

There are numerous types of spaceframe connectors [12], [13] and can be categorized into three main connection types: with a node, without a node, and as prefabricated sections. This study will focus on spaceframes with node connectors. The nodes determine the direction and angle of the bars, which in turn transfer loads axially between the joints, and typically require a fastening mechanism that connects the two. The majority of commercial space frame systems utilize proprietary joint systems and require sophisticated processes to manufacture. Mass produced systems are generally complex and could benefit from accessible fabrication methods. The joints should be repetitive, mass produced, simple to fabricate, and able to transmit all the forces in the members interconnected at the node [13].

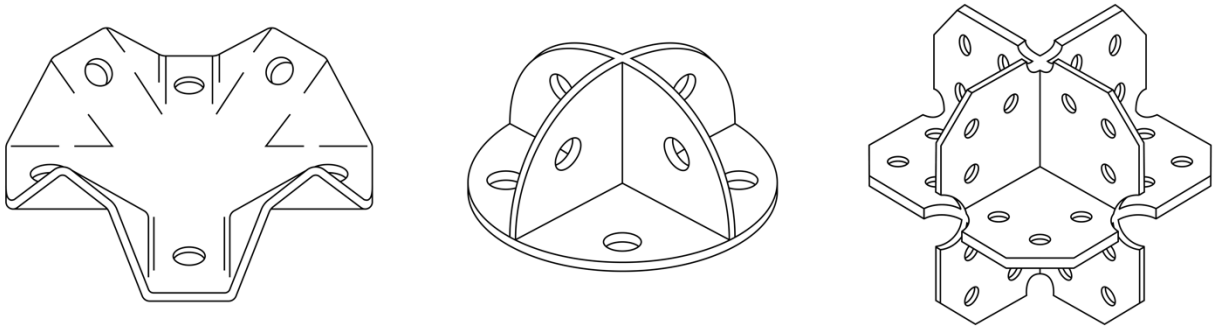

Figure 1-4: Types of octet connectors (L – R). Unistrut [14], Octatube [15], and Gyrotron [4]

There are a few examples (figure 1-4) of joints for the octet spaceframe that are simple to fabricate. The Unistrut system uses a stamped plate that interfaces with a c-shaped strut channel. As a truss system, it has been characterized extensively [14]. The Octatube system uses flat plate that are welded orthogonally and has a more "utilised image" [12] in comparison to the popular spherical node [16]. Both the unistrut and octatube systems are used as truss connectors, which only require eight connections per node ($Z = 8$), whereas a multi-layer spaceframe would have twelve connections per node ($Z = 12$). Similar to the welded plate of the octatube node, the joint used in the Gyrotron mirrors the flange at the equator and provides sufficient connections for a multi-layered octet spaceframe. The Gyrotron uses three holes per connection to fix the rotational moment of the strut.

1.3. Materials

Steel will be the material used for the joints, struts and fasteners of our octet spaceframe. Steel alloys are used in architecture particularly due to exceptional strength-to-weight ratio, durability, and versatility. Steel's specific strength means that it can support large spans with less material, allowing for the structure to be both lightweight and efficient. The octet lattice also experiences a combination of tensile and compressive loads, and steel performs well as a tensile material. Steel is also favored for its high rate of recyclability. Another traditional choice for spaceframes is aluminum because of its lightweight and corrosion resistance, although its expense typically precludes its use in building structural systems. Struts for octet spaceframes have been known to be made from timber (Satterwhite, Huybers [4]), bamboo [17], composites [15] and concrete.

It is worth mentioning the prevalence of the octet geometry in nature. The carbon atom's valency of four is tetrahedral, and as such many of its allotropes including diamond and graphite are *fcc*. Recent advances in graphene take advantage of the electromagnetic properties that emerge from

multi-layered stacks of this geometry [18]. Because of their primality, *simplices* are also found in the most fundamental corners of physics, including particle physics [19], black holes, spacetime [20], and entanglement [21]. In biology, we find abstracted similarities in protein [22], the building blocks of life. The geometry's ubiquity can be attributed to its compactness, efficiency and savings in weight. Modern applications in material science are typical as an enhancement to continuous materials, resulting in structural foams, other micro-engineered materials and metamaterials. The properties of cellular solids with octet geometry have been extensively characterized both discretely and as a continuum [2], [23]–[25].

1.4. Approach

The goal of this research is to exploit the varieties of multi-layer and multi-scale forms that an octahedral-tetrahedral spaceframe can accommodate, and to develop an accessible building method that allows individuals and small groups to construct these configurations. Computation can be used to expand the potential of forms available and improved fabrication techniques can enable that potential. Improving accessibility in the design phase can help to ensure that buildings and structures are easier to construct and modify. The use of prefabrication and modular construction can reduce construction time and costs, making projects more accessible to a wider range of individuals and communities. Our investigative approach focuses on synthesis as our primary methodological concept, where we start from defined principles such as the octet geometry, a specific steel alloy, and off-the-shelf components. Only basic arithmetic and algebra is employed to enumerate the characteristics of the system. Imperial units of measurement are used as the material and tools available conform to North American standards. We demonstrate a simple and repeatable method to build and configure an octet spaceframe.

2. Background

With a series of simple operations one can achieve a complex three-dimensional lattice in space. We look at the shapes, opportunities and profundities of this primal geometry. The tetrahedron is interpreted as the *unit cell* from which derivative polyhedra and other forms can emerge. There are a few processes the designer can adopt to produce the octet lattice, for example, the subdivision of the tetrahedron leads to the generation of the lattice and its vertex. Some basic terms and dimensions for the structure are defined.

2.1. Synthetic Geometry

From a set of rules in Euclidean space, we can derive geometric shapes and properties. With basic constructions, fundamental elements can form complex polyhedra, fractals and self-similar shapes.

2.1.1. Simplex

The triangle describes some extremal conditions. In two-dimensional Euclidean space, it is the minimal polygon and also demonstrates maximal rigidity. In three dimensions, the minimal polyhedron is the tetrahedron, and can be generalized to every spatial dimension as the *simplex* or as *tétraèdre généralisé* [26]. Both the triangle and tetrahedron have an antithetical relationship to the circle and sphere respectively. The triangle is the most discretized polygon with three edges at its boundary, and if we increase the number of points and edges, their edge lengths become infinitely small and the boundary becomes a continuous line as we approach the circle (figure 2-1). This relationship also works in three dimensions as the points of the inscribed tetrahedron rest on the surface of the sphere, and as one increases the number of points and edges of the inscribed polyhedron, we can also approximate the sphere.

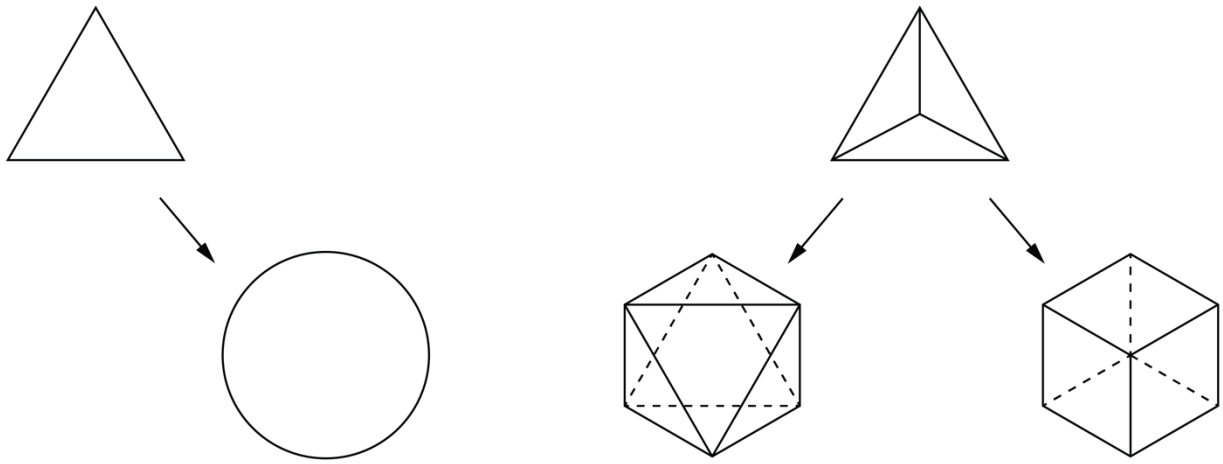

Figure 2-1. Simplex properties (L – R): From discrete to continuous polygon. Tetrahedron is fundamental to both octahedron and hexahedron.

Additionally, the octet lattice can be expanded to approximate the shape of the sphere if both share the same center which occupies the origin (0,0,0). Starting with a cuboctahedral layer surrounding the origin, subsequent layers are repeatedly added producing a spherical-like polyhedron called the *waterman polyhedron*. The waterman polyhedron is defined by the convex hull of the lattice that is a specific radius from the origin [29] which is a multiple of $\sqrt{2}$. As the

radius increases, the lattice becomes relatively denser and the convex hull approaches a smoother sphere surface, built from discrete single-length lines.

The regular tetrahedron can have each edge divided by an integer (figure 2-2), producing a combination of smaller tetrahedra and octahedra which compose the octahedral-tetrahedral lattice [27]. This three-dimensional honeycomb has the advantage of each edge being equal in length, which can be treated as the radius of a sphere, and the points of the lattice marking the coordinate system for the optimal lattice [28].

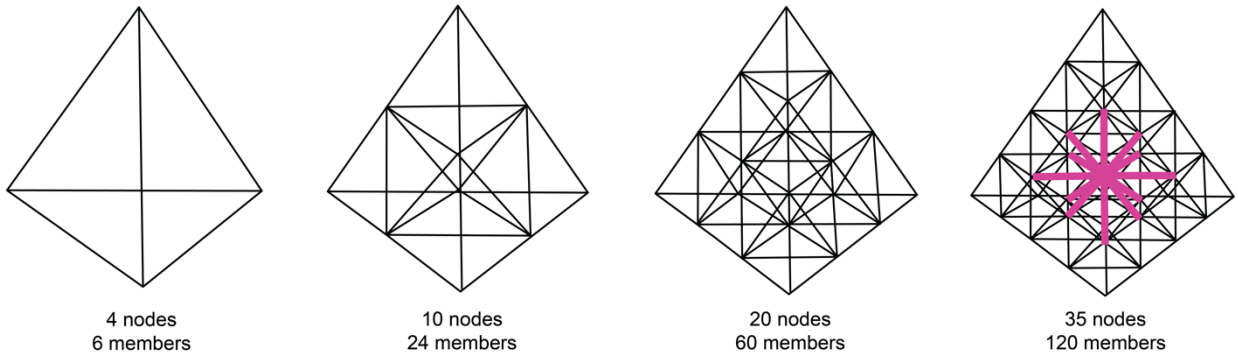

Figure 2-2: Edge lengths of the tetrahedron can be divided. Order-2 reveals the intersection of the cartesian planes as the square equators of the octahedron. The order-4 reveals the Z=12 vertex (purple).

2.1.2. Unit Cell

Because of these properties, the concept of the unit cell is reframed around the *unit tetrahedron*, whose relative edge length scales by $\sqrt{2}$. By convention, the unit cube is inscribed by a tetrahedron of $\sqrt{2}$. We can renormalize the single-length edge of the tetrahedron to be 1, rather than $\sqrt{2}$ (see Table 2-1). The lattice can be analyzed at different relative densities (figure 2-3), the first two orders giving corresponding results [1],[23]. One method involves the unit cube consisting of multiple layers, in order to achieve a few nodes with Z=12 connectivity [1].

Description	*Definition*	*Metric*
Edge length	shortest vertex to vertex	1
Triangle altitude	edge midpoint to vertex	$(\sqrt{3})/2$
Tetrahedron altitude (t)	face to vertex	$(\sqrt{6})/3$
Octahedron altitude (t)	face to face	$(\sqrt{6})/3$
Tetrahedron altitude (s)	edge midpoint to edge midpoint	$(\sqrt{2})/2$
Octahedron altitude (s)	vertex to vertex, or diagonal of unit square	$\sqrt{2}$

Table 2-1: Renormalized dimensions of tetrahedron and octahedron to unit edge length rather than $\sqrt{2}$.

The octahedron is four times the volume of the tetrahedron of congruent edge length, and half the volume of the tetrahedron of double edge length [30]. The octahedral unit cell adds a vertex on the square faces of the enclosing cube, subdividing the tetrahedron, and increasing the relative density. These dimensions and figures of the octet lattice's core geometry can be referenced by the designer to internalize and visualize the pattern. Apart from the lattice's relative densities and rescaling of metric, it can also be viewed and analyzed from different orientations.

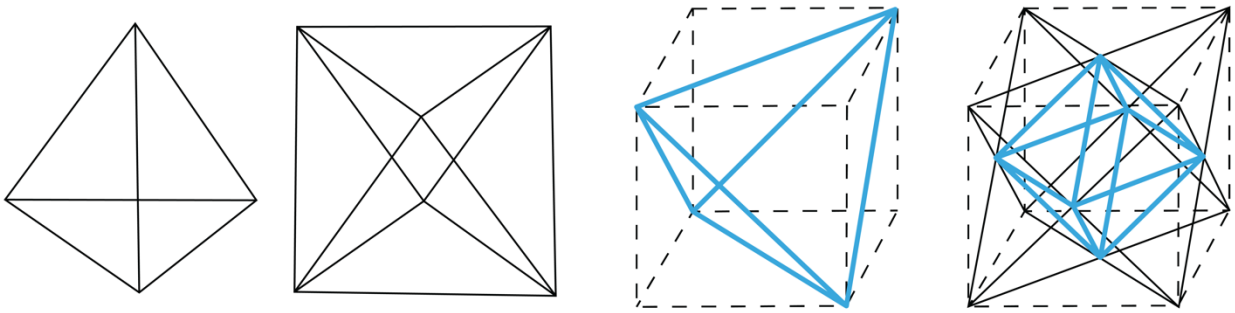

Figure 2-3: Tetrahedron and octahedron of unit edge length (left) and tetrahedron of $\sqrt{2}$ edge length and octahedron of $(\sqrt{2})/2$ edge length (right).

2.1.3. Orientation

The octet lattice has two orientations of which a planar surface can rest on a horizontal surface. We can rotate the lattice so that either a plane tiled with triangles is parallel to the XY plane, or that a plane tiled with squares is parallel to the same XY plane. We will refer to these two orientations (figure 2-4) as the *triangle orientation* and *square orientation,* respectively. The naming convention is useful for the designer when representing or thinking of the lattice in *plan* view.

Square Orientation. In the *square orientation*, the lattice has two-dimensional square grids stacked at $(\sqrt{2})/2$ intervals, at half the altitude of the octahedron. An advantage of the *square orientation* is that the coordinates for the joints are integers and use the common coordinate system *x, y, z*. However, only half of the Z_3 (cubic) integer points are used, i.e. only the points whose coordinates add up to an even number [28]. This means that for coordinates (x, y, z), if $x + y + z$ equals an even integer, then the point described is part of the *even square-oriented* octet lattice. A dual orientation of the same lattice can be made with the other half of the Z_3 points if they add up to an *odd* integer. Because of this the orientation has the benefit of square faces being parallel to the XY, YZ, XZ planes and the edge lengths are equal to $\sqrt{2}$.

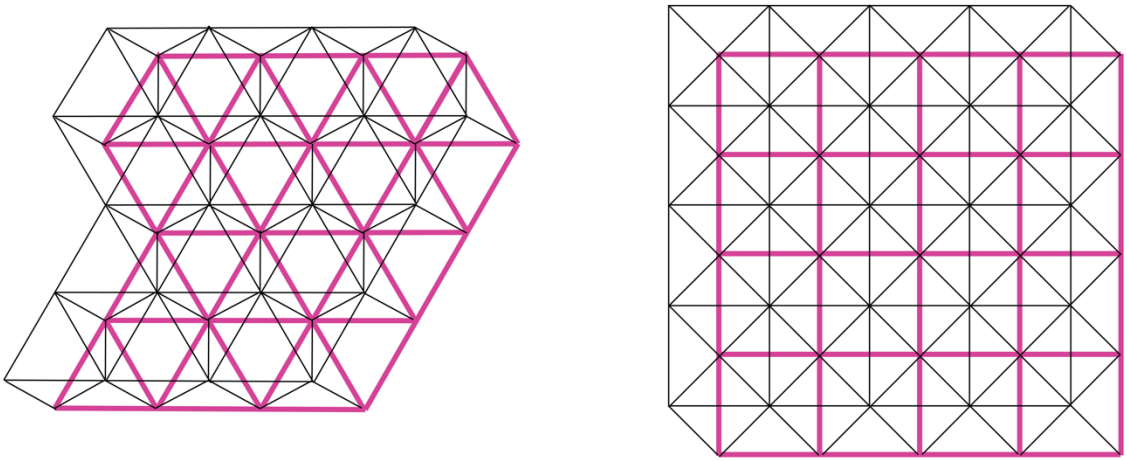

Figure 2-4: Two octet lattice orientations, plan view with two layers (L – R): triangle orientation, square orientation.

Triangle Orientation. The *triangle orientation* of the lattice with the triangular face-down on the XY plane is considered to be the fundamental orientation [27], and there is a mechanical performance advantage [2]. The spaceframe is only isotropic from a geometric perspective but mechanically performs anisotropic dependent on direction of load, favorably for the triangle orientation. This orientation can be created by stacking triangulated layers in an "ABCABC..." arrangement [23]. However, the coordinates of the vertices of the lattice are more difficult to account for, and are multiples per table 2-1.

2.1.4. Emergence

Fuller described the geometry of the three-dimensional simplex lattice as the *isotropic vector matrix* [27] emphasizing that each radial length from a central node is the one and same to the edge on the surface of the cuboctahedron, the *vector equilibrium* [30]. Emergent [31] from the geometric properties described, Fuller states that the octet demonstrates the characteristic of *synergy*; referring to the "behavior of whole systems unpredicted by the behavior of their parts taken separately" [32]. These ascribed emergent qualities to the lattice can be interpreted in two ways: as phenomena which can be mechanically observed in the performance of the structure, or as a means from which the shape generates itself [33].

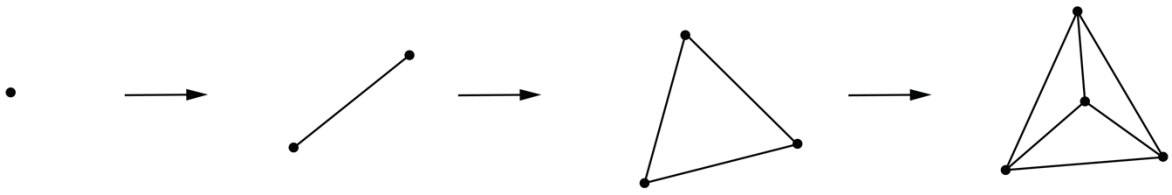

Figure 2-5: Simplex in dimension zero to three. The rule for the subsequent generation is to add one point and completely connect the graph with lines.

2.1.5. Shape Grammar

A shape grammar is a set of visual rules from which a simple shape can be elaborated into a complex pattern [34] and can generate designs such as the octet geometry. A grammar can decompose a design by beginning with a set of shapes and defining the relationships between them. As shown in figure 2-5, a tetrahedron can be generated procedurally by iterating through the dimensions of the simplex: from point, line, triangle and up to the tetrahedron at the third dimension. The tetrahedron can then be subdivided into the lattice (figure 2-2), hence the grammar of the octet point cloud can be implemented through two rules. The lattice is a tiling in three dimensions, similar to how the equilateral triangle tiles the plane, and the order of the lattice, or relative density can be increased by a similar arithmetic rule as shown below. As we will explore, the design of the components of the lattice (joints, struts and fasteners) can be controlled parametrically and is a good candidate for shape and cost evaluation per [35].

2.2. Lattice Properties

The octet lattice has some properties due to its single-length geometry, which can be employed for building stiff and interesting looking structures. The lattice is capable of both multi-layer and multi-scale subdivision, terms which are described below. We can also make use of arithmetic properties of the lattice to help enumerate its elements.

2.2.1. Multi-scale

Multi-layer lattices are produced by repeating rows of elements where two or more lines converge in space, and the tiling of the respective plane produces a grid pattern. These tiled planes are stacked as layers at regular intervals. We can call the visual appearance that emerges the *parallel effect*. Multi-scale lattices demonstrate symmetry at different edge lengths, producing self-similar polyhedra of different sizes. We can call this visual feature the *fractal effect*. The octet lattice demonstrates both of these hierarchical properties.

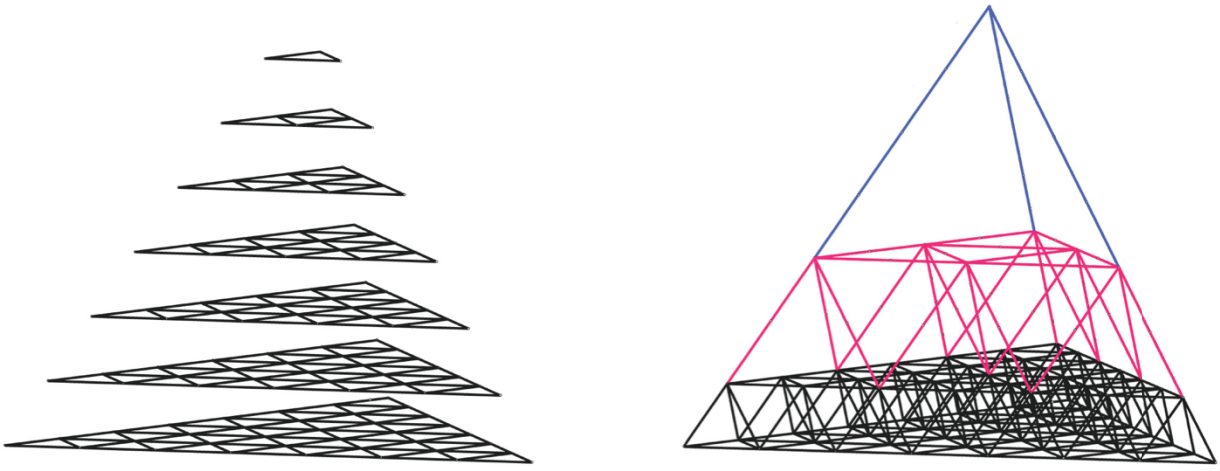

Figure 2-6: Multi-layer (left) and multi-scale (right) lattices, demonstrating the parallel and fractal effect respectively.

2.2.2. Recursion

Recursion is the process of repeating items in a self-similar way. As the lattice is similarly situated, it can be broken down into smaller shapes that are repeated and combined to create a final form that is similar to the original configuration. This process can continue multiple times, creating increasingly complex shapes with intricate patterns. In the octet system, regular polyhedral forms can be derived from the *schafli* family of {3,3},{3,4} and its dual {4,3}.

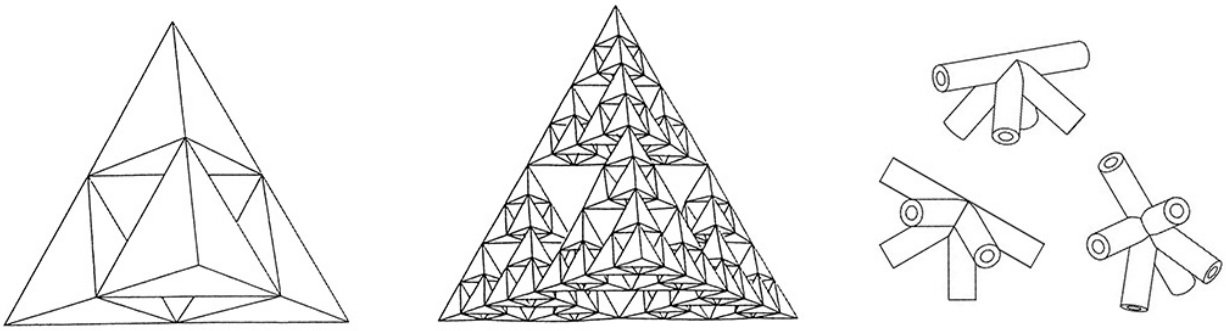

Figure 2-7: Sierpinski Tetrahedron. Order-2 and 4 recursion [36], with discrete edges and deep holes persistent (left). Connectors designed by the author with Z=6 (right).

A *sierpinski* tetrahedron can be produced using an iterated function system or a recursive *chaos game* method [36], to generate an octet lattice with our same connector. However, this is not always useful, as the point cloud generated leaves large *deep* holes, and produces smaller *shallow* holes with each iteration (figure 2-7). A stochastic point cloud could also be produced using the same procedure, but only approximates an octet lattice after many iterations. This method is less appropriate as we lose any coherence and do not maintain equal distances between points.

2.2.3. Arithmetic

The *arithmetic triangle* has numerous emergent properties not discussed here, including the binomial theorem, central limit theorem, the normal distribution, and combinatorics [37].

```
1  1  1  1   1   1   1   1   1   1  1 1
1  2  3  4   5   6   7   8   9  10 11
1  3  6 10  15  21  28  36  45  55
1  4 10 20  35  56  84 120 165
1  5 15 35  70 126 210 330
1  6 21 56 126 252 462
1  7 28 84 210 462
1  8 36 120 330
1  9 45 165
1 10 55
1 11
1
```

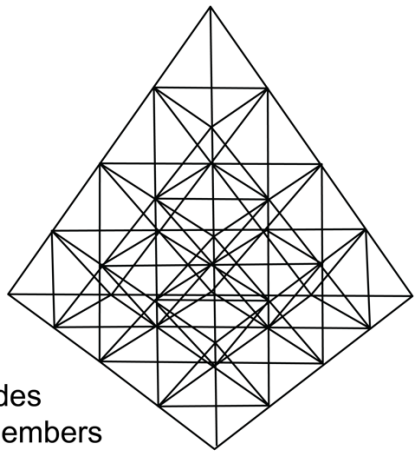

Figure 2-8. Arithmetic triangle enumerating vertices of order-4 tetrahedron.

The sequence generated by the triangle [38] can enumerate characteristic features of any n-dimensional *simplex* at any order of division. In our case, the vertices and edges of any multi-layer tetrahedron can be discerned. The arithmetic triangle is the coordinator for the integer lattice [39] and indexes the total number of vertices of any tetrahedron-shaped octet lattice.

Vertices of the lattice. The rows of the triangle index the divisions of edge length (offset by $m + 1$), and the 4th column of the triangle (index also offset by $n + 1$ dimension) lists the tetrahedral numbers [40], see figure 2-8. The equations below are all dependent on the variable m, the order of the tetrahedron or triangle.

$$Te_m = j_m = \frac{m(m+1)(m+2)}{6}$$

As each slice of the tetrahedron is a triangle that is also tiled, the triangular numbers can be used to count sequential layers, reducing the value of m at each subsequent layer.

$$T_m = \frac{m(m+1)}{2}$$

Edges of the lattice. To find the total number of edges of an order-m tetrahedron, we first find the $(m - 1)$ number of vertices of the prior tetrahedron, or one lower order of tetrahedron. Using the equation for the number of vertices, we can multiply by 6 which is the number of edges of the order-1 tetrahedron.

$$b_m = 6j_{m-1}$$

Substituting the tetrahedron equation for (j_{m-1}), the 6 is cancelled:

$$b_m = m(m-1)(m+1) = m^3 - m$$

As such for base tetrahedral forms of any order, we can determine the number of connectors and struts that we require. We can extend this method beyond forms of the tetrahedron and include the series of octahedral, cuboctahedral, truncated cuboctahedral, and stella octangula numbers, which are all forms produced with the octet lattice. These figurate numbers can also be used subtractively to describe the cavities that take these forms within the structure.

2.2.4. Rigidity

Spaceframes have a load carrying mode that is three-dimensional. Structural and weight efficiency are achieved by concentrating the constituent material along narrow lines, rather than spreading it continuously to fill space [25]. Considerable work has been done on the effective properties of cellular microstructures [2], [24], [41] and the lattice has been extensively modelled as a continuum [42]. Open-cell foams provide an appropriate analogy for our study of macrostructures. When triangulated frames are loaded, the struts in a spatial structure support axial loads that are tensile in some and compressive in others [41]. Stretching dominated structures are stronger than bending dominated structures.

A *sufficient* condition for the deformation of a periodic structure to be stretching dominated is that the unit cell (i.e. within a cube) of the structure is statically determinate. Maxwell [43] developed an algebraic rule for a pin-jointed frame of b struts and j joints that will determine whether the structure is static. [23] The criterion in three dimensions is stated as:

$$b - 3j + 6 \geq 0$$

where b and j are the number of struts and nodes, respectively, in the unit cell. [41] further showed that sufficient and *necessary* condition for the structure to be stretching dominated is that the connectivity, or *valency*, at each node is Z = 12. If more than 12 struts connect at one node, the framework is redundant from a rigidity standpoint. This condition is equivalent to the connectivity of the octet lattice, and at least pertaining to cellular microstructures, it is conjectured [41] that it is close to the optimal single length-scale structure in regards to rigidity.

2.2.5. Collapse

The octet spaceframe collapses by elastic buckling of the struts according to Euler's critical load [23] of the column, as given by:

$$P_{cr} = \frac{q^2 \pi^3 E a^4}{l^2}$$

Tubes outperform solid rods primarily through the reduction of weight and the equation can be adjusted appropriately [44] for tubing. Once sufficient strain is achieved, the critical load reaches a value equal to the material stress, and this is when the tube buckles. The remaining variables represent the tension/compression modulus of the material, the area moment of inertia and length of the member. Given a network of struts, the factor q determines the rotational stiffness of the end nodes of the strut, and is dependent on the buckling mode. The lattice may buckle in many different modes and the resulting problem is "very complicated" [23] to analyze completely. The problem can be simplified by assuming that the struts are pin-jointed (similar to how spherical and threaded nodes perform) and the rotational stiffness of the nodes is zero (n = 1) in the equation. As such, pin-jointed connections are utilized for finite element analysis.

The compressive behavior of foam-based or 3D-printed octet lattices has been analyzed in different loading directions [2]. The results are not *omni-rational* [32] demonstrating anisotropy in the structural performance. The shear strength of the spaceframe is periodic [23], with respect to rotations of 60-degrees about the three axes and varies by less than 10%, with the shear strength at maximum for a 30-degree rotation: in its *triangle-orientation*.

An understanding of the octet lattice's geometry and properties will help us internalize the space in which we can work. The use of basic dimensions and the ability to manipulate both multi-layer and multi-scale qualities can give the designer options to create diverse configurations of the spaceframe. The arithmetic triangle and some generative techniques will be used to produce and enumerate the lattice.

3. Methodology

The methodology used integrates the needs of the designer, fabricator and builder into a process that would enable multiple spatial configurations and intentionally simplifies fabrication and assembly. There are multiple approaches to generate these configurations that embrace both analog and digital tools. Some of the above-mentioned methods can be applied to generate the lattice in a computational environment. The designer can also imagine and ideate different forms that the structure can take by employing synthetic methods such as drawing and modelmaking. We then apply the appropriate scale for human use, material choice, and further enhance our theme of minimal and optimal structural hierarchy.

3.1. Design

The choice of geometry and type of spaceframe has already constrained the design solution to a structure that is minimal in terms of variability of parts, and with necessary and sufficient conditions for rigidity and stiffness. The design of the system should enable a diversity of configurations, be easily scalable, and facilitate community participation. The components should be affordable, use simple tooling and make use of off-the-shelf components when available. In practice, the designer can account for user needs and preferences, and can use participatory design processes that involve end-users in the concept generation process, ensuring that their perspectives are reflected in the final design. This approach can lead to more responsive designs that better meet the needs of those who use the space.

3.1.1. Modelmaking

Modelmaking is a quick and intuitive way to explore the realm of spatial possibilities. The stick and ball category of model is familiar in molecular chemistry. This form of modelmaking allows for improvisational form-finding and hands-on exploration without the constraint of a virtual interface. The designer is able to view the model from multiple angles, and rigidity is tangibly experienced. The tactility of physical modelmaking is in contrast to computational approaches, which are non-tactile. There are some shortcomings of the physical modelmaking method: first a kit must be produced, and a surplus of parts are required for full exploration of the space. The models cannot be easily shared or iterated with other people remotely, and cannot be analyzed structurally outside the computational environment.

Different modelmaking kits are produced from craft materials (figure 3-1). The kits are designed for high throughput and can be produced with digital fabrication tools such as a lasercutter or 3D printer. No fasteners are used in the kits and rely predominantly on friction or snap fits between pieces.

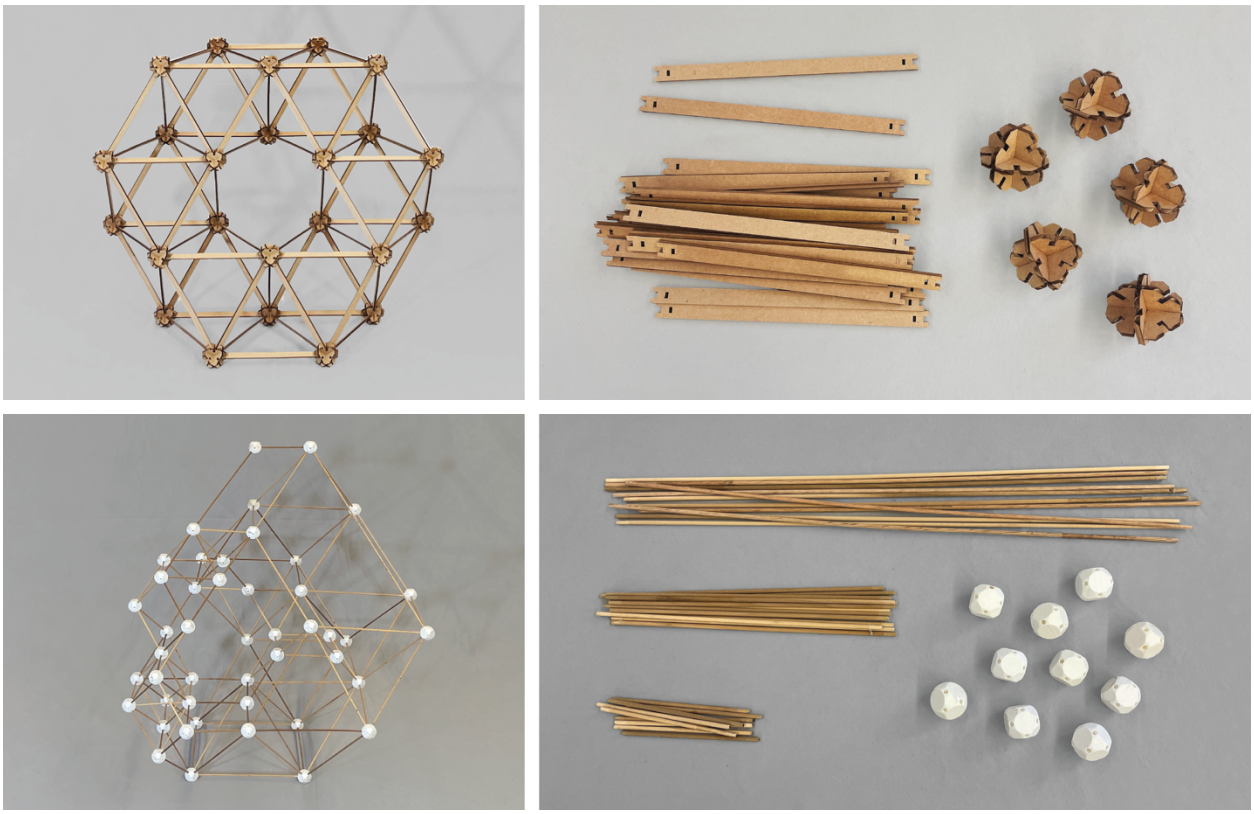

Figure 3-1: Octet model kits. Torus (top) from a two-layer truss and single-length system. Cardboard connector kit with one size of strut and snap connections. Model (bottom) of a multi-layer and multi-scale octet spaceframe, with three orders of strut length. 3D-printed PLA connector kit with different lengths of wooden dowel.

3.1.2. Participatory Design

This project intends to encourage the individual to take an active role in creating, repairing, and modifying their own structures and architecture. Kits, like the examples above, can be used to stimulate discussion and generate designs in a group setting. Design direction can be given by prompts or objectives, such as trying to build a tower or a bridge (figure 3-2). Goal-setting and decision-making are integral to the design process. Group dynamics involved in creative and collaborative problem solving can be explored. Models can be built with design intent, or alternatively the potential of the space can be explored subtractively. Some advice is provided by Satterwhite in exploring the octet design space, that it is “simpler to assemble the full dense grid, and then subsequently to remove the unwanted structure, at each level, to form the required voids” (Satterwhite [4]).


Figure 3-2: High school students creating towers with cardboard octet connector set (images courtesy of Keith Lee and Adam Burke).

Our primary design requirements are constrained to that of human anthropometric and ergonomic needs. Components can be appropriately sized to be handled, moved and constructed by a single person. As such weight and dimensional qualities of material will be limited so as not to injure the individual from lifting, carrying items small distances, or from repetitive strain from frequent tasks. We must also develop an approach to fabricate the elements of our structure that are accessible to non-experts. Fabrication processes can be limited to a few methods that can be applied in most fabrication shop environments without specialized equipment.

At minimum, smaller structures should be able to be constructed by an individual. A group build is proposed as an effective method of building larger structures. With a minimal skill prerequisite, a few individuals can come together to erect a structure using collective effort. An intuitive system that is also easy to assemble and repair can increase a community's self-sufficiency and sense of empowerment by erecting their own structures. This method, akin to that of a barnraising, allows for the pooling of resources and knowledge, making the construction process faster and more efficient.

3.1.3. Computational Tools

Digital tools like CAD are useful for designing components and assemblies, and are used here for modelling variants in a virtual environment. FEA is used for the evaluation of spaceframes due to the program ability to process and analyze structures efficiently. Computation is used to determine physical conditions that a spatial structure may be subjected to, enabling designers to identify potential issues and optimize their designs accordingly. Simulation provides buckling analysis by decomposing the object into a discrete mesh of a determined size and makes use of Euler's critical load (see 2.2.5). Digital fabrication enables CAD to be post-processed as toolpaths which enable numerical control of precision equipment such as a waterjet.

Point Cloud. We generate a point cloud of the octet lattice using Rhino and Grasshopper (McNeel), with the application of different parametric methods. Three methods of producing octet coordinate points are described (figure 3-3):

Tetrahedron. The no-core method produces a tetrahedron with the square orientation. By projecting a triangle of increasing size from the origin, the boundary of a tetrahedron is created, but the inside points of the projected face are missing. However, this defect only starts to occur at $m = 3$, and that the first missing vertex is at $(2,2,2)$. Note: the missing vertex is also the nucleus of the first hexagon. If the projected tetrahedral shell is restarted at even occurrences, i.e. $(2m, 2m, 2m)$, the lattice is created. The count must decrease $m - 2$ for each cone to result in a tetrahedral shape.

Transformation. Methods to generate the octet truss through symmetry operations such as reflections, rotations and translations are explored by [45], [46]. As shown above, an apparent way is to take the grid of tiled triangles, and rotate each successive layer by multiples of 120-degrees. While the cited examples are confined to two-layer spaceframes, the same method can be applied to multi-layered spaceframes.

Stacking layers. By generating a series of real numbers, a 45-degree line can be projected out onto the XY plane in four directions from the origin, producing the square orientation. With uniform increments in the z-axis, we can stack layers in an "ABAB..." offset. For a triangle orientation, we create a grid and stack layers that adhere to the tetrahedral dimensions per table 2-1, and the layers are offset in triple "ABCABC..." arrangements.

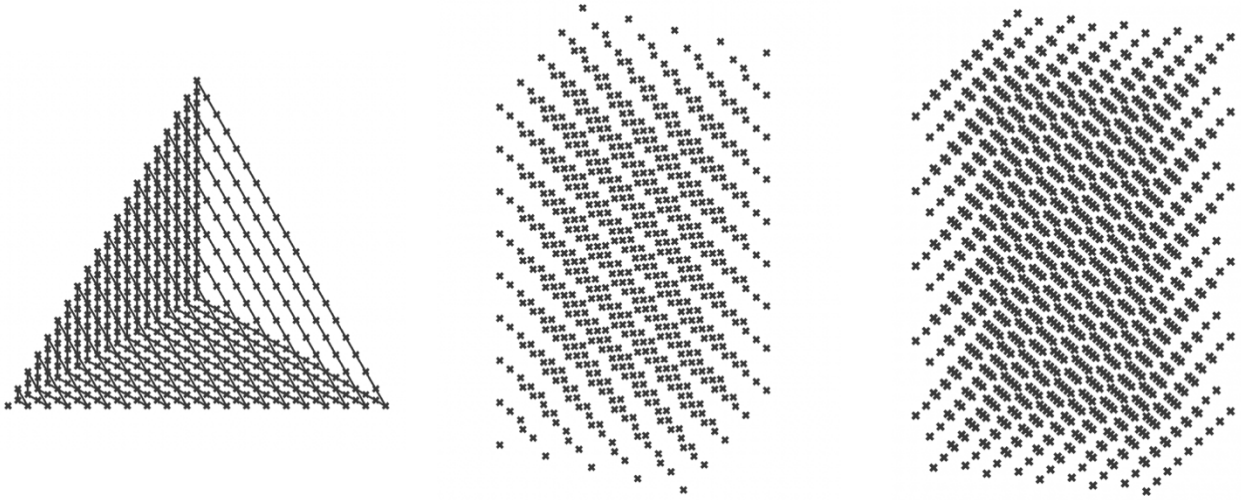

Figure 3-3: Point clouds generated in Grasshopper (L – R). Tetrahedral shell, square-orientation, and triangle-orientation.

3.1.4. Fabrication tools

We can frame the fabrication of the components of the octet structure through a few lenses. Decisions on the scale of the elements are dependent on the human ability to manipulate them and the skill level of the labor involved in making the components. Similarly, a material choice can be made on structural properties, cost and availability. We discuss the decision of using commercially available off-the-shelf (COTS) cross-bracing for struts and adapting them for our application. As such, we need to consider materials that are cheap to produce and procure, and will last as a durable good.

Steel. As a highly recycled and recyclable material, it is a good choice to reduce end-of-life waste and environmental impact, and its durability allows for multiple cycles of reuse without significant wear or degradation of the qualities of the material. Though the initial carbon cost of steel can be high, it is a demonstrated participant of the circular economy. The durability and weather resilience of a steel alloy can be further enhanced by a surface protective treatment including galvanization or a powdercoat.

As a design decision, we can choose steel for its specific strength and performance characteristics but it also achieves some other metrics. Steel is affordable, and is a commoditized cost with availability in most economic regions. As described below, there are many COTS architectural and construction products that are commercially available, which we can repurpose for our use. Steel is also easier to weld for a novice.

Batch production. Batch production strategy is utilized. Unit cost of components should be low, which presents a challenge without the economies of scale that come with mass-production. Additionally, tooling and capital costs should remain low to increase accessibility of the method to more people. The material volume of each batch can be limited to fulfill the quantities required for the chosen design, or to batches appropriately sized for the budget. A preference for manual shop tools is given, such as simple presses for cost and accessibility reasons, but exceptions are made for tools that increase production efficiency.

Early prototypes of struts based on a design by [47] were made from ¾ inch EMT steel conduit, conventionally used to house and route electrical wiring. The conduit was affordable and the ends were malleable enough to press in a manual screw press. At three-foot lengths, the tubing could support a human weight, however this approached the limit of the tubing before plastic deformation. As such, an increase in wall thickness and OD of tubing was necessary. At Z=12, there are also a considerably large quantity of struts per unit of node, and reducing the requirement to fabricate each strut would reduce the effort of the design-builder.

Off-the shelf. As such, a strategy for strut fabrication includes using COTS products, to reduce the effort of making the largest unit of strut. Tubing with two ends formed, flattened and punched, is a common type of strut that can be found commercially at various lengths. We look for lengths at common material dimensions. Ideally we can find a family of struts with a few sizes, as different lengths have different utility to human scale, material economy, and can help us produce the fractal effect seen in the models.

3.2. Detail

The spaceframe system will consist of three types of components: joints, struts, and fasteners. We design a simple gusset type joint using CAD, with intersecting plates on the XY, YZ, and XZ planes, and the origin as the center of the lattice vertex. Struts are identified from the scaffolding industry that inform the dimensions of the joint.

3.2.1. Joint Detail

Regarding choice of type of connector, two important issues are the tradeoffs between acceptable aesthetic and reasonable costs [12]. In our case the aesthetic is utility at the human scale at the design, fabrication and construction phases, which aligns well with the mission of keeping unit costs low. The cuboctahedral vertex can be produced by the intersection of three square plates,

the orthogonal profile of which will be convenient when it comes to handling and workholding during fabrication. The plates intersect with a lap-joint as shown in figure 3-4.

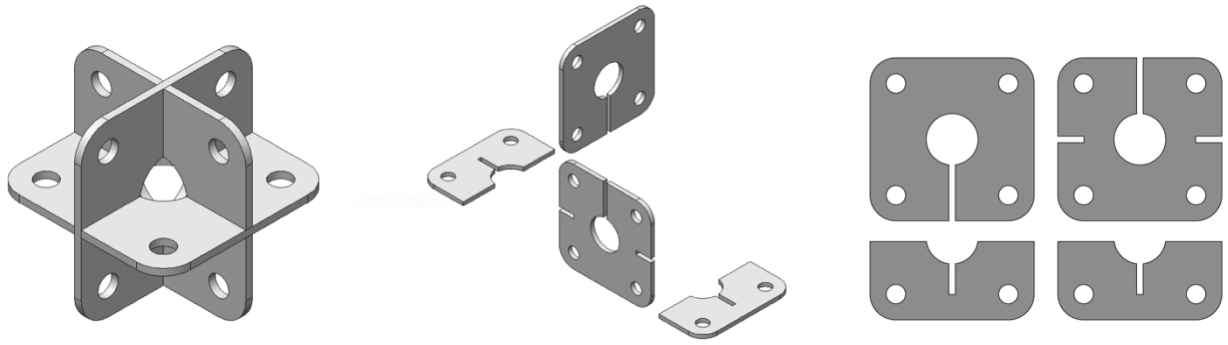

Figure 3-4: Octet Joint (L – R). Plates assembled, Exploded View, and Flat Pattern.

The design of the joint is parametric, dependent on three variables: material thickness, hole size, and diagonal offset. Diagonal offset is the diagonal of the square face, and results in the hole-to-hole distance across the face. This offset is derived by the designers intended dimension from center of the node to the center of the next node, or the scaled unit distance between points in the octet point cloud. Once a strut is chosen, this nominal distance is the sum of the hole-to-hole strut length plus the hole-to-hole diagonal offset. Additionally, a relief hole at the center of the node is added to reduce weight and provides the option of another attachment point. The corners of each plate are filleted, using the centers of each connector hole as the origin and determinant of the radius.

3.2.2. Strut Detail

Characteristic for all spatial structures, regardless of connector type, is that the member ends are worked [12]. We repurpose a component from the scaffolding industry and have found that steel cross-braces are very appropriate for our application. Cross-braces are conventionally used to enhance the stability of the scaffold by increasing rigidity and distributing the weight of the scaffolding evenly across the structure. Each cross-brace comes at a nominal length and is made up of two struts joined at the middle by a retaining bolt, allowing the brace to expand into an x-shape. This bolt can be removed with a $7/16^{th}$ inch wrench. The struts have a standardized profile and are endformed, including flattened at the ends, with a hole and rounded profile punched. Using a commoditized product allows for higher throughput and volume of component whilst minimizing effort and cost.

Description	Bay Length	Bay Height	Hole-to-Hole	Nominal Length
7 x 3 Cross Brace	84”	36”	91.39” (7’ 7 3/8”)	96”

Table 3-1: Dimensions of 7x3 cross-braces.

This solution works for a nominal 8ft dimension between nodes, and 6 struts will produce an 8ft edge length tetrahedral cell of the lattice. However, we require other sizes to produce the fractal effect, particularly strut dimensions that are half or double of the nominal length (figure 3-5), but accounting for the offset of the joint width. As such, a fabrication method to alter the length of the braces must be developed. Sheet goods in the construction industry are commonly sized at 4x8ft as a standard dimension.

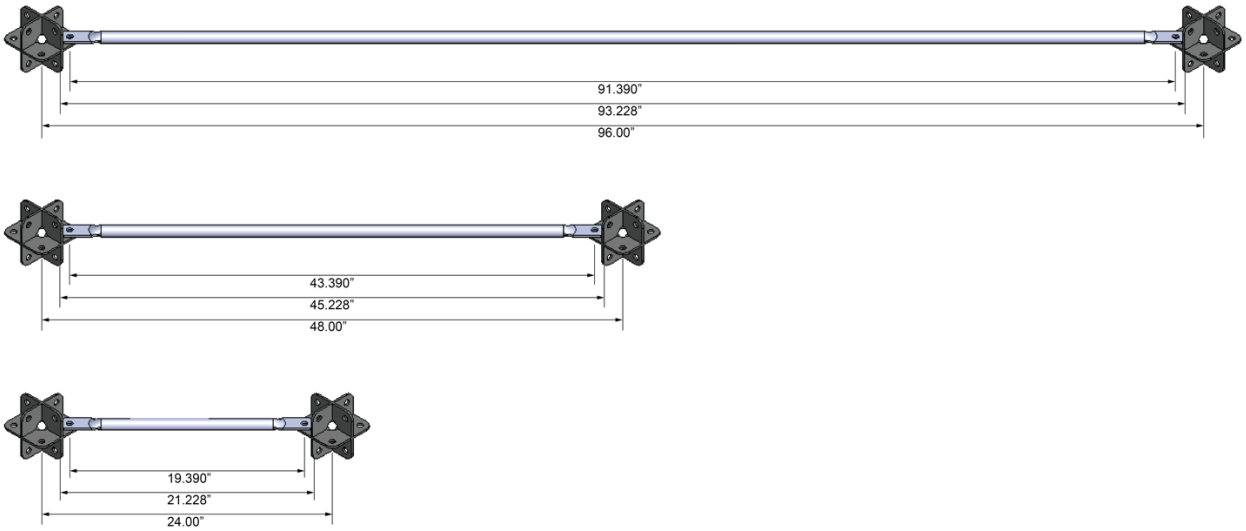

Figure 3-5: Strut dimensions for nominal 8ft, 4ft, and 2ft units (Top to bottom). Hole-to-hole length, cut length and nominal length.

3.2.3. Fasteners

The number of fasteners (bolts, nuts, washers) required is a function of multiplying the number of struts by its two ends. Fasteners used are rated grade 8 for high tensile strength, and are specified to ½"-13 coarse thread and flake galvanized. Washers or locknuts are not included for simplicity. The joint and strut self-describe its assembly process: holes are made to receive fasteners to secure the joint to each of the members, which have holes of the same size. The joint is full when $Z = 12$, and the lattice will be less stiff when $Z < 12$. The square orientated planes are more susceptible to rotational moments.

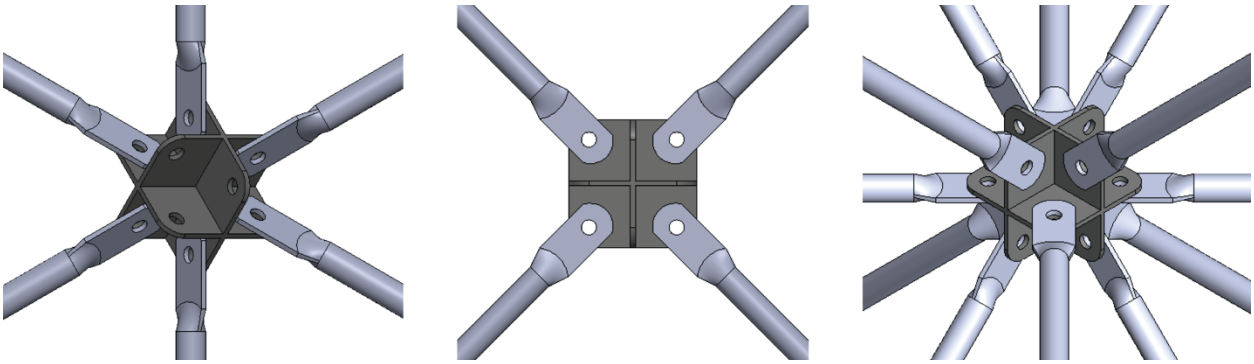

Fig 3-6: Assemblies centered on joint (L – R). Triangle orientation, square orientation, fully connected with $Z = 12$

3.3. Concept

Through modelmaking and generative methods, various test structures were proposed and evaluated based on certain considerations. These criteria include a reasonable quantity of components, a design that could demonstrate the multi-scale member length with both fractal and parallel effect, a modest footprint and some height restrictions. The winning design (figure 3-7) showed consideration of the footprint and chose an 8ft octahedral envelope. The concept model gives us the minimum quantity of components for our kit.

3.3.1. Concept Model

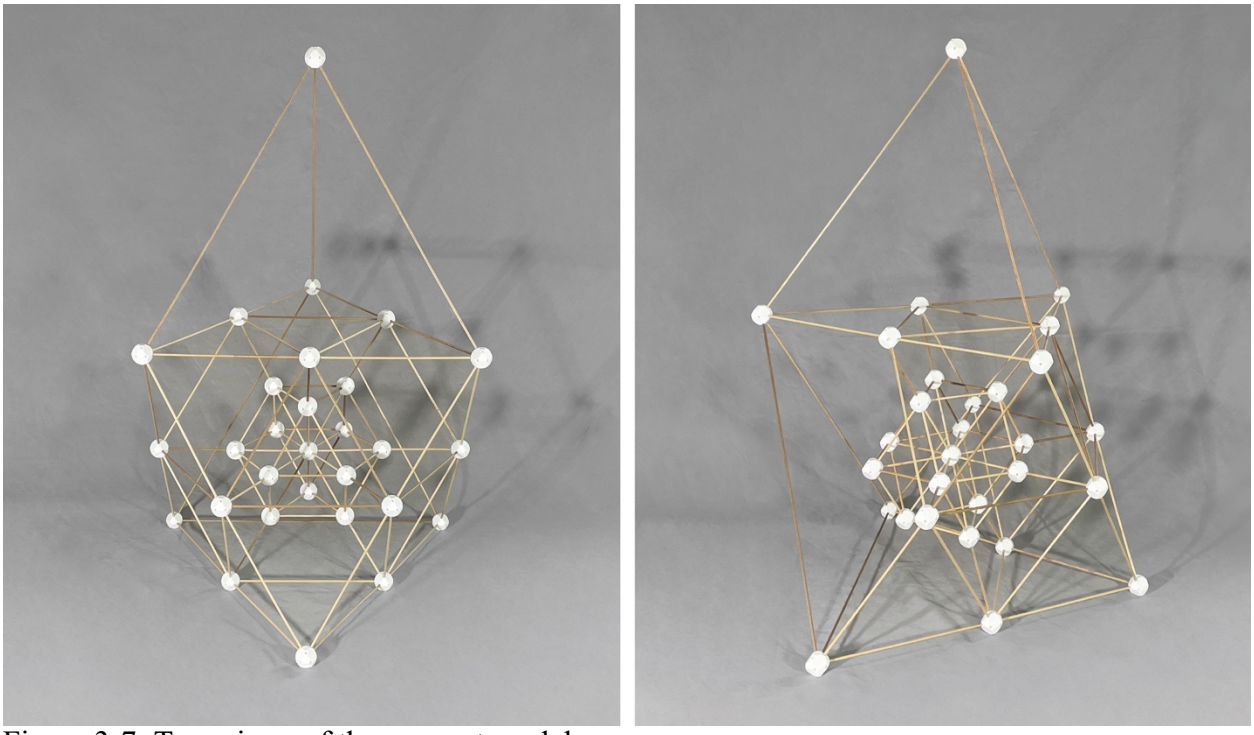

Figure 3-7: Two views of the concept model

The octahedron subdivides to order-3, revealing a cuboctahedral nucleus made of 2ft struts. We remove three of the 4ft struts that help suspend the nuclear cuboctahedron, allowing it to cantilever. An 8ft tetrahedral cell caps the base octahedron, bringing the structure to a 13ft height. A combination of enumeration techniques used in section 2.2.3 can be used to count the elements needed:

Component	*Quantity*
Octet joint	29
8ft strut	6
4ft strut	33
2ft strut	45
Bolt	168
Nut	168

Table 3-2: Quantities of each component for concept.

As shown, we can get two 4ft struts from one 8ft strut, and four 2ft struts from one 8ft strut. As such, 34 struts are needed, which means we procure 17 cross-braces. Each type of fastener (nut and bolt) can be calculated by multiplying total number of struts by two.

Using the triangle-orientation point cloud from section 3.1.3, we can create a virtual model of our concept, which will aid us in analyzing the mechanical performance of the lattice.

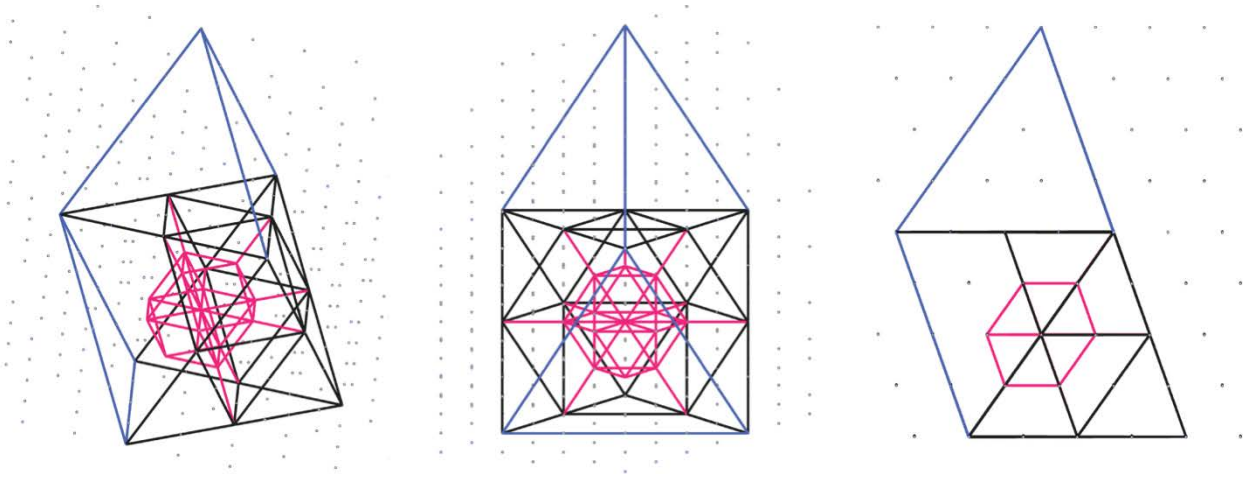

Figure 3-8: Digital model of the concept, with strut lengths highlighted in different colors.

3.3.2. Finite Element Analysis

Here we will share results from FEA of the spaceframe using both Solidworks 2021 (Dassault Systemes) and Rhino / Grasshopper (McNeel). Because of imperfection effects in the physical material [48], the simulations will over-estimate peak load and a safety factor must be added. The cases analyzed here all have the lattice in the triangle orientation. We are interested in collecting data that will characterize the building system. We also model the above concept, and try to understand the tensile and compressive forces that the physical structure will experience.

Buckling Cases. Using Solidworks FEA, we analyze the force required to buckle our base case 8ft tetrahedron and octahedron when the load is directed towards the ground and applied at the nodes. The tetrahedron has only one joint at its summit vertex from which the load is applied, and some variation in direction is explored. The octahedron has three vertices among which the load is applied in different combinations. Both the tetrahedron and octahedron have three-way symmetry, so we can analyze the range from 0 – 60 degrees, see figure 3-9.

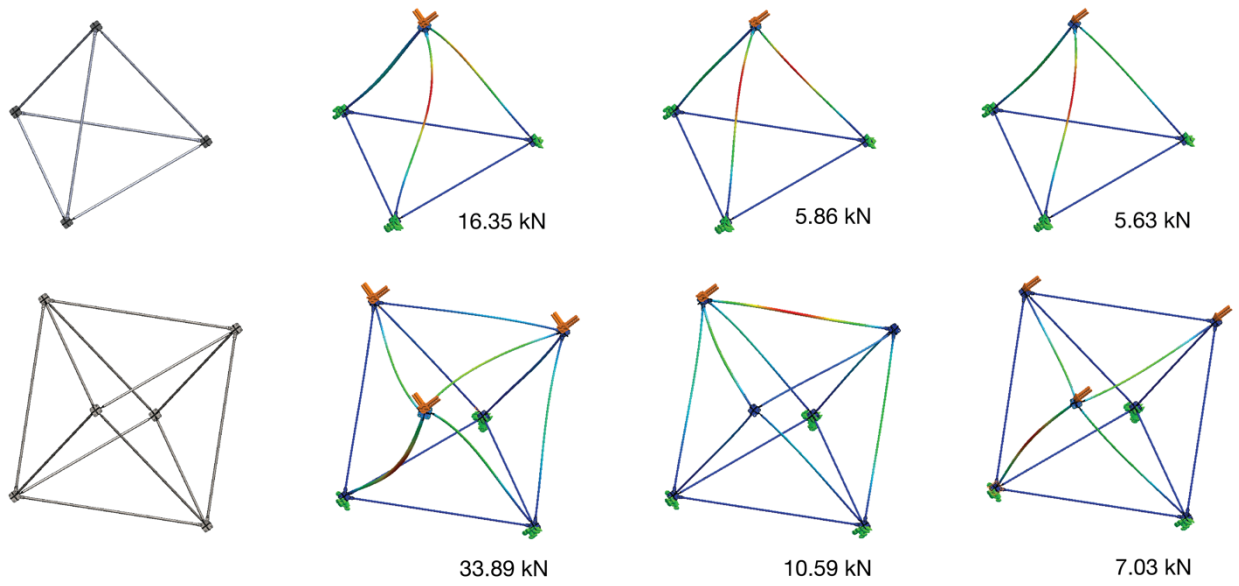

Fig 3-9: Critical buckling occurs with loads applied at top nodes (orange vector) of 8ft tetrahedra and octahedra. Nodes at bottom are fixed points (green). The second case from the left demonstrates an idealized loading case, where force is applied evenly across the node and the resultant load is Normal to the ground. The third and fourth cases demonstrate variation from uneven loading in different directions. Visual deformation is scaled up by 20%, and a heatmap along struts show amplitude of deformation. The solid element model has a mesh seed size of 4in max.

Elasticity. The members of the octet lattice experience either tension or compression when other members are loaded. Since the structure will initially be assembled by individuals, it is critical to understand how different configurations perform with a human weight present. The assembler can move about the structure freely, and the conditions will change throughout the structure. We analyze the concept configuration with a human moving throughout the structure in figure 3-10. Visual deformation is scaled up by 10%. It is clear that the structure is stiffer and more resilient when the live load is spread out over multiple nodes and rather than concentrated in the middle of a horizontal strut.

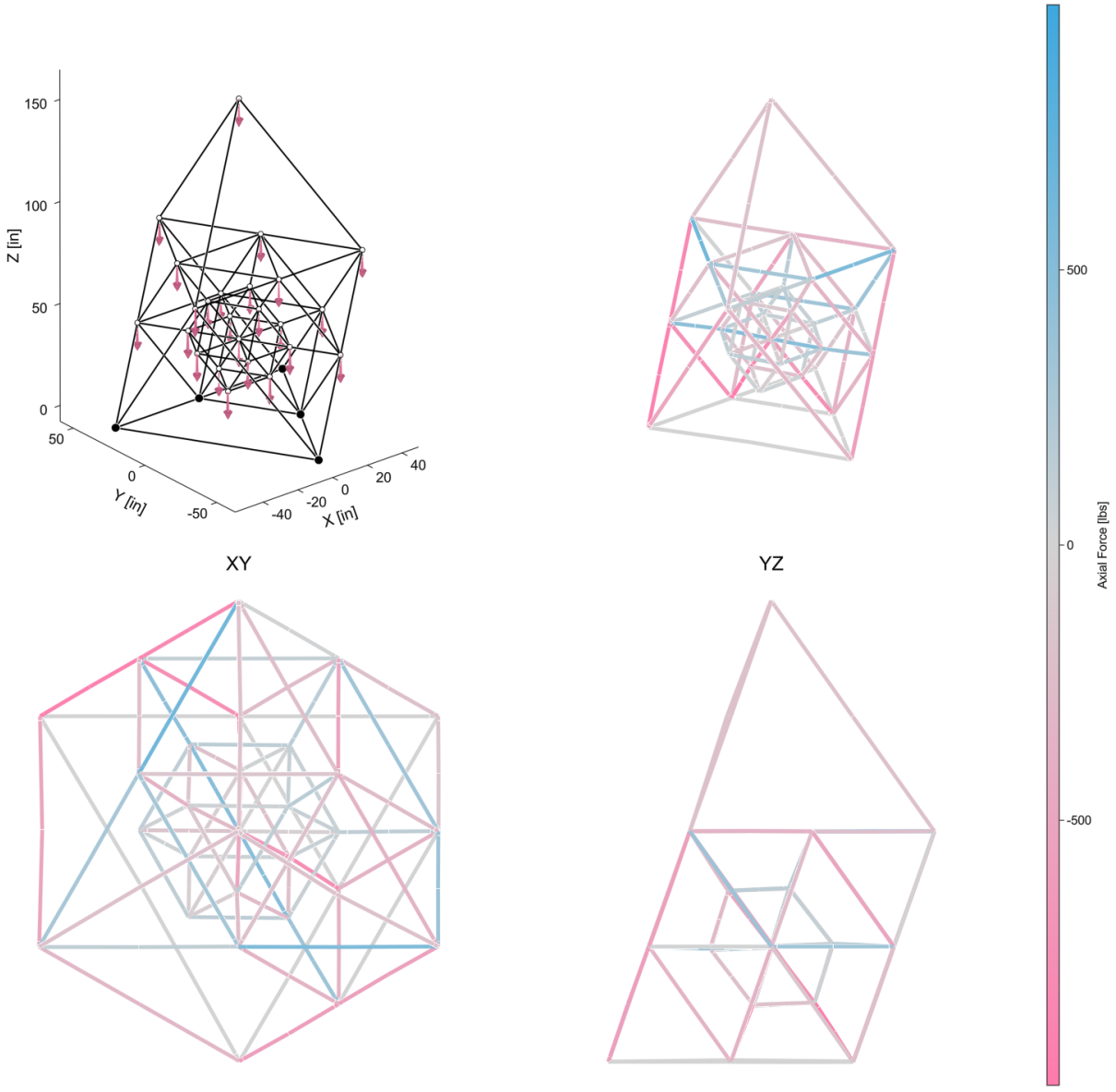

Figure 3-10: Finite Element Analysis. A linear elastic FEA model was performed (courtesy of Keith Lee) to simulate structural behavior under climbing loads. Each strut was modeled by 4 beam elements, with nodes at the ends of the flattened connection region and at the center of the strut. A 100kg load was distributed over two points spaced 6" apart to simulate two feet. This load was placed at the quarter points of each strut to observe the overall deflection behavior. Negative axial force shows that a strut is under tension (blue) and positive axial force shows that a strut is under compression (red).

4. Results

Multiple configurations of an octet spatial structure are built using a constrained kit of parts, starting with the concept above. Multiple people are involved in the assembly process. Plastic deformation is encountered on certain 8ft struts. The components of the kit are fabricated using accessible metalworking equipment, and repurposed cross-braces are modified for multiple strut lengths. We share some of process involved, including unit costs of the components.

4.1. Fabrication

Fabrication techniques involved are accessible to non-experts with little experience, but require access to certain machines and equipment. Tools used are a mix of digital fabrication and basic tools in a shop. A die press is developed to flatten the ends of the struts and to make use of an ironworker. Skills such as welding can be learnt or outsourced.

4.1.1. Joint Fabrication

The joints are fabricated from 3/16 inch hot-rolled sheet of common A36 steel alloy. At 7.65lbs per square foot, we constrain the dimension of delivered plate to 2x2ft to limit weight at 30.6lbs for an individual to move. A flat vector for each A, B and C plate (figure 3-4) is exported from CAD, nested to 6 units per plate, and a toolpath is generated to cut the material.

Waterjet. The computer-controlled OMAX waterjet (2652) uses a high-pressure jet of water mixed with an abrasive granular material to cut a 2D pattern in a wide range of material and thickness. Other precision 2D computer-controlled metal cutting technology like laser or plasma-cutter would be suitable, but a key benefit of the waterjet is that material is submerged in water and does not absorb as much heat during cutting, minimizing the risk of warping or distortion in the material. The abrasive used is a consumable that needs to be accounted for as each unit of joint uses about 14lbs of 80 grit garnet, and takes approximately 15 minutes per cutting cycle.

Plate Assembly. The component plates are transported flat, and assembled prior to welding. The tight tolerances provided by the waterjet can make a welding jig unnecessary, and ± 0.01in tolerance added to the width of the lap-joint is found to allow for a swift and stiff assembly with a mallet and block of wood. For looser fitting assemblies, the plates can be squared relative to each other with a simple jig made from two trued aluminum cubes. The cubes are fastened to opposite corners before welding, with the effort of adding and removing the jig added to the cycle time.

Welding. The plates are TIG welded together to produce a unit joint (figure 4-1). Each joint has 24 internal corners where the plates meet at right angles, and requires 48 tack welds and 24 bead welds. The tack welds help the plates to not move or distort as the steel heats up from continuous welding. The C plates are first tacked to the A plate, and then the lap joints where the A and B plates intersect are tacked. The tack welding brings the assembled joint up to a suitable temperature (300 – 500F) to easily weld beads.

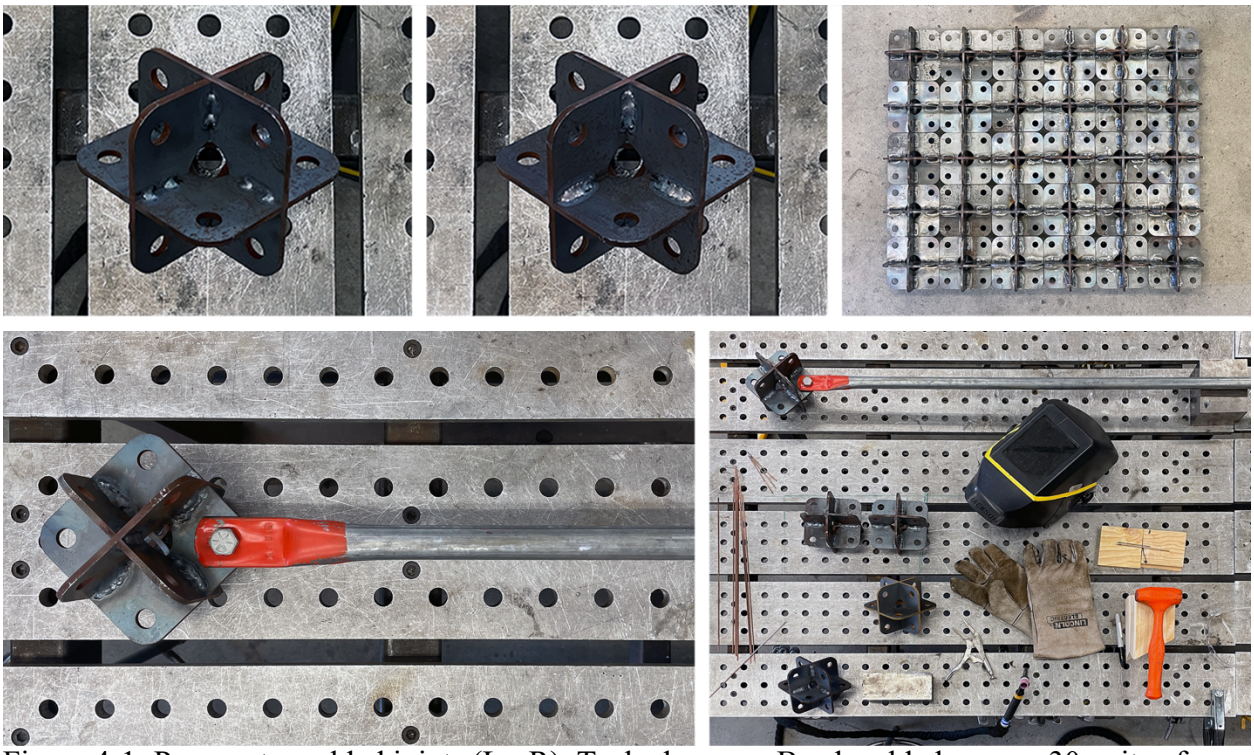

Figure 4-1: Process to welded joints (L - R). Tacked corner. Bead welded corner. 30 units of joints. Test fit onto strut. Welding set-up and equipment.

The joint has 8 orthogonal cavities with 3 corners each. The joints absorb a significant amount of heat and radiate (500F – 700F) after a few cavities are welded. It is suggested to weld two units of joints at a time, switching to the other once a few cavities are welded on the prior. The current used on the TIG is set at 160-200A DC, with good results found using 3/32in tungsten and 3/32in filler rod. 2ft of filler rod is consumed per joint, corresponding to the average welded bead length of 1 inch. Cycle time is approximately 35-45 minutes per unit of joint for a novice welder, including time to assemble and prepare materials. The joints are finished with a polyester powdercoat.

4.1.2. Strut Fabrication

Beyond the 8ft length, other dimension of struts need to be produced. Tubing ends can be worked with a variety of presses, including and not limited to an arbor press, screw press or hydraulic press. While these are common and cost-effective shop tools, cycle time and throughput is not very high and a larger load at a few tons is required to press our tubing ends.

Tooling. A universal flattening tool was developed that could be moved between different types of presses. The tool required a vertical action of $>$ 1in to accommodate a tube of the same diameter. The interchangeable dies are made from steel blocks, and were milled square to form the ends of the struts. The flattening dies feature a curved profile and a stop at the rear for uniform endforming. Steel bars with mounting points sandwich the dies and ride on ½” OD dowel pins on sleeve bearings. To enable a return action, die springs were used at a medium load rating of 145lbs/in.

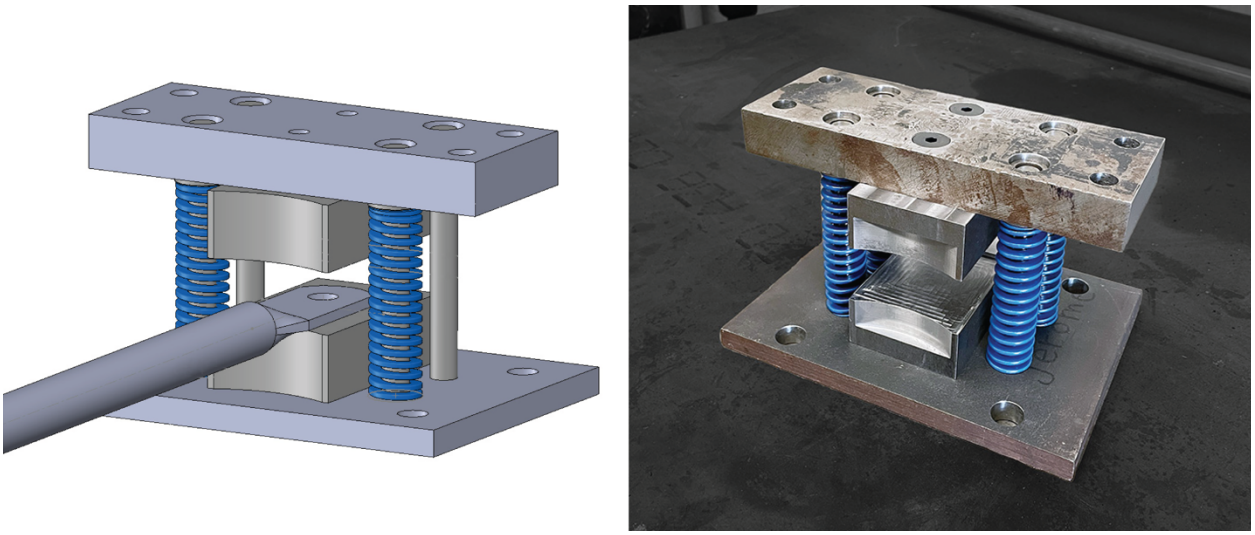

Figure 4-2: Flattening tool (L – R). CAD of tool design. Fabricated and assembled tool.

Ironworker. An ironworker, a press that uses a hydraulic lever to cut metal is commonly used for quick end forming of tubing, and is versatile as a tool. An appropriate die would provide both flattening and punching. The rounded edge can be achieved with an additional tool with a knife edge, or can be nibbled on another station of the iron worker. As the braces are galvanized, they do not require a finishing process.

The hole can be formed in a variety of ways including punched by a die with sufficient load, or the hole can be drilled out. In either situation, the distance from hole to hole is paramount to the integrity of the multi-scale system. For that we build a jig that uses a pin and an adjustable distance to ensure our struts are of adequate length; the first hole is the reference for the second hole. We drill out the hole using a drill press and a tungsten 9/16th in hole saw. The placement of the hole should stay somewhat centered on the flattened profile.

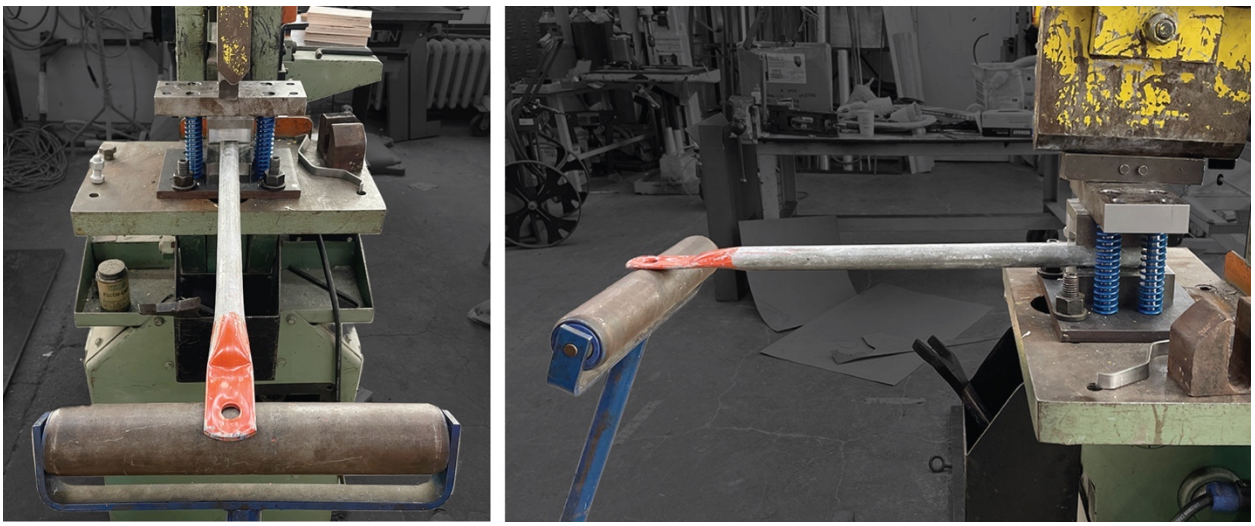

Figure 4-3: Strut flattening. Hydraulic press (Piranha 50-ton ironworker), flattening tool and die.

4.1.3. Unit Economics

The table below summarizes the cost per unit joint, for a batch production volume of 30 joints. The cost of consumable is excluded for both waterjet and welding operations, and are included in the pre- and post-operations of receiving steel plate and powdercoat finishing respectively. The labor costs for both waterjet and welding operations are assumed based on a $30/hr rate, and are included.

	Description	*Process*	*Time/mins*	*Material/$*	*Labor/$*	*Main Consumable*
1	Delivery of plate	Mill to Truck	-	6.4	-	Energy, Fuel
2	Flat design cut	Waterjet	14	-	7.5	Garnet, Water
3	Welding of plate	TIG Weld	35	-	17.5	Filler Rod, Shield
4	Protective coating	Powdercoat	-	6	-	Polyester Powder

Table 4-1: Summary of fabrication methods – per unit joint

The table below summarizes the cost per unit 8ft strut, for a batch production volume of 48 struts. Material cost of 2ft and 4ft struts are fractions of the 8ft strut, plus the operations 2-4 per end that needs to be formed. The cost of consumable is excluded for the endforming, though it is worth mentioning that the holesaw to drill out the holes cost about $7 and are only capable of 40 holes before end-of-life. The labor costs are assumed based on a $30/hr rate.

	Description	*Process*	*Time/mins*	*Material/$*	*Labor/$*	*Main Consumable*
1	Delivery of brace	Mill to Truck	-	8.5	-	Energy, Fuel
2	Cut to length	H. Bandsaw	<1	-	0.5	Electricity, blade
3	Flatten	Ironworker	<1	-	0.5	Electricity
4	Drill Hole	Drill press	2	-	1	Drill bits

Table 4-2: Summary of fabrication methods – per strut

Set-up time for these processes are externalized. Capital costs of procuring and operating the machinery are excluded. Because the components are reusable and modular, the cost per unit is amortized over multiple structures and service cycles.

4.1.4. Kit of Parts

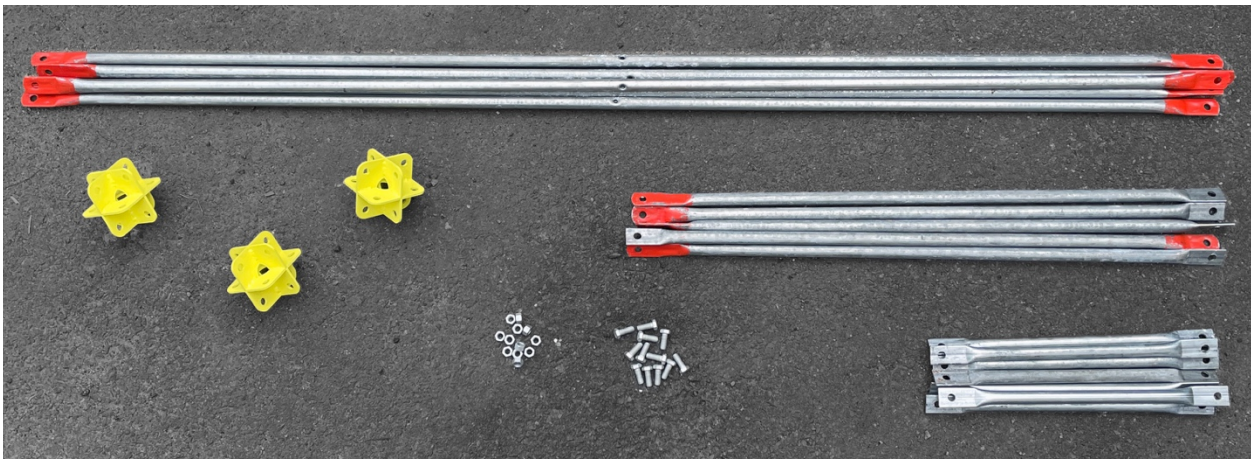

Figure 4-4: Elements of the kit of parts consist of 8ft, 4ft, and 2ft struts, octet node, ½ inch bolts and nuts.

The joints, struts and fasteners were aggregated into a kit of parts (figure 4-4). Transportation of the kit to a site requires some consideration with larger volume of components. Milk crates are useful for transport of joints, and plastic wrap is handy for packaging struts together. A few 8ft lengths of strut, just like 2x4 framing studs, can be transported through the length of most sedans and non-compact passenger vehicles. Alternatively, they can be strapped to the roof of passenger vehicles with a roof rack. A dolly is useful for moving components over shorter distances.

The table below summarizes the cost of producing a kit of parts. The kit was sized with the concept in mind, with a small surplus of 4ft and 2ft struts and a large surplus of the 8ft struts for further experimentation. The costs include the labor rate as discussed in section 4.1.3.

Description	*Unit Weight / lbs*	*Unit Cost / $*	*Kit Quantity*	*Kit Cost / $*
Octet joint	3.0	37.4	30	1122
8ft strut	7.0	8.5	24	204
4ft strut	3.4	6.3	36	227
2ft strut	1.6	4.4	48	211
Bolt	0.1	1.0	200	200
Nut	0.04	0.7	200	140

Table 4-3: Unit weight and cost, quantities and cost for the produced kit of parts, totaling $2104.

We further examine some of the base configurations of the system. In use the cost per node is dependent on the number of struts involved, hence the connectivity is important. The cost of different amounts of connectivity for one joint are shown in the table below. One set of fasteners is allocated per connection. The Z=6 configuration can be used as a rough proxy for costing the spatial system.

Connectivity	*Description*	*Cost / $*
Z=3	minimal rigidity	68
Z=6	planar or edge condition	98.6
Z=8	truss condition	119
Z=12	fully connected	159.8

Table 4-4: Cost of configurations per node, assuming joint plus 8ft bar per connection.

For a maximally packed space with Z=12 (figure 4-7) throughout the structure, we can calculate the cost based on the volume of components. We return to the concept of the tetrahedral unit cell as a discrete unit of mensuration and use arithmetic methods (section 2.2.3) to count components. As the tetrahedron is a 1/3rd the volume of the cube it is inscribed within, we can convert to cubic feet but would need to account for surface and edge conditions and duplicate elements. The table below summarizes the cost per 8ft, 4ft and 2ft packed tetrahedral lattices.

Description	*Cost per tetrahedral foot / $*
8ft strut	3.7
4ft strut	10.1
2ft strut	37.2

Table 4-5: Cost of spatial structure by volume, packed with different lengths of strut.

4.2. Assembly

Several configurations of the structure were erected at the N52 courtyard outside the MIT Architecture woodshop. The courtyard constrained the footprint of the built structures, and has a level asphalt surface. This was the first validation of the different strut lengths and the tolerances required as more layers were added to the structure.

4.2.1. Build One

The first structure built is from the concept model resulting in a 13ft tall tower sitting on an 8ft triangular base, and took under two hours to assemble with two persons worth of labor (figure 4-5). The stick and ball model from figure 3-7 was brought to the site as a reference. It was useful to orient the model in the same direction as the structure being built. The structure was erected from the ground up, layer by layer starting with 2ft intervals.

Figure 4-5: Sequence of build one. Following the concept model, the assembly order is based on human intuition. Time to assemble is under two hours.

4.2.2. Assembly tools

A few simple tools are needed for assembly. A 3/4in socket wrench or driver coupled with a another 3/4in open wrench was used to fasten the ½”-13 bolts and nuts together. At minimum, two adjustable wrenches would suffice, though the open wrench is preferred. Multiples of each tool should be procured for a group build. Fasteners are first hand tightened until a significant number of elements are connected, or until the structure needs to be climbed. Each connection has up to an 1/8in of movement, and premature over-tightening of fasteners can lead to difficulty fitting struts further down. A resolution is to loosen adjacent connections before proceeding

further, but should be considered rework. Once completely assembled, every connection on the structure should be retightened to a specified torque.

4.2.3. Build Two

Next builds attempted improvisational form-finding. By subtracting nodes and struts from the previous configuration, we can reduce redundancy and attempt to expand the structure in another direction. Also, components from overly stiff areas can be reallocated to other sections of the structure that needs reinforcement.

Figure 4-6: Build two. The structure is extended by removing nodes from overly stiff sections and reusing them elsewhere. Multiple individuals contribute to the assembly.

Although robustness was simulated in FEA, plastic deformation was encountered at the midpoint of the 8ft struts positioned at the top of an octahedron. The struts deformed via bending under one human weight when walking across the horizontal strut. Each strut had a hole from where the retaining bolt held the braces together, and it is along the axis of the hole that the deformation occurred. A solution was found (courtesy of Eduardo Gascon Alvarez) by replacing the bent strut with an intact cross-brace, hence two struts rather than one. The geometry of the two flattened ends of the struts sandwiches the gusset of the joint nicely. This provides a further opportunity

for the linear analysis of a design, which could identify members that are under bending moments and require reinforced braces for specific sections.

4.2.4. Participants

People were invited to participate in group builds held on different days, and contribute to both the design intent and assembly. Anecdotally, one participant was keen on building in a certain direction to optimize the use of available space. Another participant attempted to build towards a nearby rooftop, using the structure as a means of access. One participant was interested in the fractal effect, and wanted to know how many levels of recursion could take place. Another participant hadn't used a socket wrench or a driver before, but was enthusiastic to learn and be involved in a hands-on activity. Most participants were excited to climb the structure and were not hesitant to check its sturdiness. Participants generally wanted to build the structure larger, and a recurring piece of feedback was that we required more joints and 4ft struts in the kit.

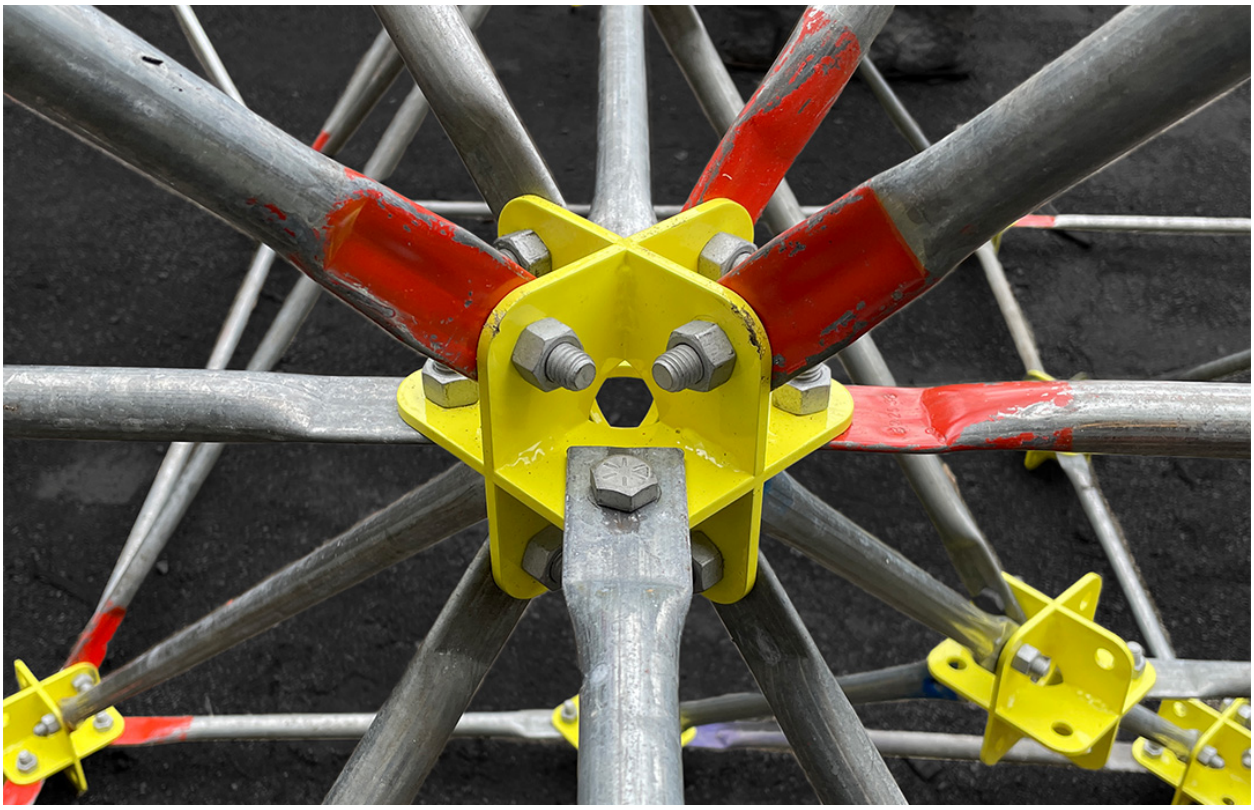

Figure 4-7: Joint detail with Z=12, from a subsequent build in the square-orientation.

5. Conclusion

5.1. Summary of contributions

Methods to produce the octet lattice geometry are compiled, and include rules for a grammar and an arithmetic technique. A point cloud is produced in CAD to fluidly design and iterate through configurations. The structural system is simplified to available and repurposed components for struts, and uses accessible methods to fabricate the joint. The system intentionally reduces cost by using steel and minimizing the number of fabrication processes required. The labor involved in both fabrication and assembly is also reduced by simplification of the component detail design. The use of 8ft struts enables integration with off-the-shelf materials from the construction industry. The system is capable of both multi-layer and multi-scale configurations through the use of multiple strut lengths, which enhances the wide range of flexibility in form. The structures demonstrated are assembled in only a few hours.

5.2. Potential impact

Results from this research produced a full scale and functional structure. Individuals and communities can use a system like this to design and build diverse structures with many different applications. The built environment is limited in form and prefabricated systems are generally orthogonal in contrast, and this system is an efficient method to produce multi-layered truss networks. There are unlimited formal possibilities, and built cases are only constrained by material performance and mechanical limits. Due to the viable cost of the fabricated components, the system can be widely deployable and multi-functional with many creative use cases.

5.3. Limitations and future work

Though these methods of construction are simple, this particular system has yet to be fully characterized both discretely and continuously, and requires further testing and validation under different loading conditions. The rotational mode of the connection between the joint and strut is a distinct part of the system that differs it from others, and requires further analysis to determine mode of failure. The decision to use one fastener per node is a function of minimization; an additional hole per connection doubles production time for every hole and doubles the cost of fasteners.

Failure modes. The hole in the center of the 8ft strut that remains from the cross-brace was not included in CAD and leads to a plastic failure mode that was not predicted through FEA. It is not advised to stand in the middle of a horizontal 8ft strut. This particular case of failure mode requires further study and more formal limits of what can or cannot be climbed or loaded. The structure is also noticeably less stiff when the joints have low connectivity. It is evident that when connectivity is restricted to a single plane, or with the reduction of Z, the frame is less stiff. Designs should consider two-layer shells and then further optimize choice of strut size. A combination cubic plus octet lattice [49] can be considered to increase stiffness by providing additional configuration options, and would increase the connectivity to Z=18 at the expense of single-length members.

Building systems. A variety of auxiliary systems, including flooring systems, insulation and cladding would need integration in order to build a habitable structure. A standoff could be fastened to the joint and used to mount these systems. Purlin stools [12] have not been fully considered as of yet, but can be accommodated in the central hole at the intersection of the

gusset. The strut length and 8ft distance between the joints was designed in consideration of framing standards and the attachment of commonly available dimensions of sheet material.

Automation. Savings in material costs and labor costs would occur with increase of volume and decrease of time respectively. Automation would decrease cycle times, manhours of labor, and unit costs but with upfront tooling and capital expenses. For joints, the cnc waterjet is already an automated process, but savings in time and labor could be found from the automation of welding. The orthogonality of the plate intersections makes these joints an ideal candidate for MIG welding. For struts, additions to the endforming die could enable hole punching and shearing of the profiles with a press. Using the ironworker to punch holes would drastically increase productivity.

Other struts. Because of the die press tool, various types of material can be used for struts. We envision that different type of profiles of stock can be used as a member, including angle iron or flat bar. Scrap material would be a good candidate for reusability, and structural analysis could allocate certain types of struts based on demand. This sort of system would embrace a diversity of strut type, but the joint could remain a standardized or fixed design.

Computational design environment. Accessible virtual tools, such as 3D graph paper, would enable the designer to explore different configurations. Accounting for sequence of assembly has its limitations in determining the order of stable configurations and intermediate loads on the structure. Stability during assembly is currently intuition-based and solvable by non-expert individuals, but continues to pose a challenge for automated processes. Computation and simulation reduces the risks in outcome, which is not as comprehensive a process with intuition alone. Interesting approaches include a hybrid of computationally generative and human decision-making in the design process.

5.4. Concluding Remarks

This thesis shows a simple method to design and fabricate an octet spatial structure. The kit-of-parts is affordable and easily reproducible because of a strategy that repurposes scaffolding as material for struts and uses accessible techniques to fabricate the octet joint. The system allows for a multi-layered and multi-scale spaceframe, whose modularity permits a vast amount of configurations.

The work also demonstrates multiple methods to generate octet lattices, particularly to produce point clouds which allow the designer to explore the space within a virtual environment. A symbiotic approach between digital and analog modelmaking methods gives the designer the ability to produce forms synthetically yet also analyze them through simulation. Assembly of the structure was demonstrated through participatory builds that involved members of the community.

In summary, this research exhibits how simple geometry produces highly modular and variable structures with very few parts, empowering the individual to affect the built environment.

6. References

[1] R. M. Christensen, “The Three-Dimensional Analog of the Classical Two-Dimensional Truss System,” *J. Appl. Mech.*, vol. 71, no. 2, pp. 285–287, May 2004, doi: 10.1115/1.1651090.

[2] Y. Li, H. Gu, M. Pavier, and H. Coules, “Compressive behaviours of octet-truss lattices,” *Proc. Inst. Mech. Eng. Part C J. Mech. Eng. Sci.*, vol. 234, no. 16, pp. 3257–3269, Aug. 2020, doi: 10.1177/0954406220913586.

[3] J. Borrego, *Space grid structures: skeletal frameworks and stressed-skin systems*. Cambridge, Mass.: MIT Press, 1977.

[4] J. Chilton, *Space grid structures*. Oxford, UK ; Boston, Mass: Architectural Press, 2000.

[5] “R. Buckminster Fuller, Shoji Sadao. Tetrahedron City Project, Yomiuriland, Japan (Aerial perspective). c.1968 | MoMA,” *The Museum of Modern Art*. https://www.moma.org/collection/works/863 (accessed Jan. 19, 2023).

[6] S. Sadao, *Buckminster Fuller and Isamu Noguchi: best of friends*. Milan New York: 5 Continents The Isamu Noguchi foundation and Garden Museum, 2011.

[7] L. I. Kahn and A. G. Tyng, *City Tower, Philadelphia, PA,1956–57, model. Courtesy of the Louis I. Kahn Collection, University of Pennsylvania and the Pennsylvania Historical and Museum Commission.*

[8] A. Sykiotis, “Philadelphia City Tower: an exploration of architectural representation through drawings and photographs of physical models,” 2022, Accessed: Apr. 21, 2023. [Online]. Available: https://repository.tudelft.nl/islandora/object/uuid%3A960ea9f5-808b-409e-8b33-c90cb1b18b05

[9] B. Auger, *The architect and the computer*. London: Pall Mall Press, 1972.

[10] Alcan, “Description of the two Gyrotron structures, Expo 67, Montréal, Québec; Canadian Centre for Architecture, Montréal; Gift of May Cutler.” https://www.cca.qc.ca/en/search/details/collection/object/423142 (accessed Jan. 19, 2023).

[11] S. Kelly, “Night view of the Gyrotron at La Ronde, Expo 67, Montréal, Québec; Canadian Centre for Architecture, Montréal; Gift of May Cutler; Architect: Sean Kelly,” 1967. https://www.cca.qc.ca/en/search/details/collection/object/415539 (accessed Jan. 19, 2023).

[12] J. M. Gerrits, “An architectonic approach of choosing a space frame system,” 1998.

[13] T. T. Lan, “Space Frame Structures,” 1999.

[14] P. H. Coy, *Structural analysis of Unistrut space-frame roofs.* Ann Arbor: University of Michigan Press for University of Michigan Research Institute, 1959. Accessed: Sep. 06, 2022. [Online]. Available: https://catalog.hathitrust.org/Record/001627169

[15] Yang Xiao, Bai Yu, Luo Fu Jia, Zhao Xiao-Ling, and He Xu-hui, “Fiber-Reinforced Polymer Composite Members with Adhesive Bonded Sleeve Joints for Space Frame Structures,” *J. Mater. Civ. Eng.*, vol. 29, no. 2, p. 04016208, Feb. 2017, doi: 10.1061/(ASCE)MT.1943-5533.0001737.

[16] J. Brütting, G. Senatore, A.-M. Muresan, I. Mirtsopoulos, and C. Fivet, Eds., “Synthesis of Kit-of-parts Structures for Reuse,” *Adv. Archit. Geom. 2020*, 2021.

[17] I. Saevfors, “Bamboo Space Frames,” *Saevfors Consulting*. http://www.saevfors.se/Space_Frames.html

[18] J. M. Park, Y. Cao, K. Watanabe, T. Taniguchi, and P. Jarillo-Herrero, “Tunable strongly coupled superconductivity in magic-angle twisted trilayer graphene,” *Nature*, vol. 590, no. 7845, Art. no. 7845, Feb. 2021, doi: 10.1038/s41586-021-03192-0.
[19] C. Quigg, “The Double Simplex.” arXiv, Sep. 05, 2005. Accessed: May 03, 2023. [Online]. Available: http://arxiv.org/abs/hep-ph/0509037
[20] C. W. Misner, K. S. Thorne, J. A. Wheeler, and D. Kaiser, *Gravitation*. Princeton, N.J: Princeton University Press, 2017.
[21] R. A. Bertlmann, H. Narnhofer, and W. Thirring, “A Geometric Picture of Entanglement and Bell Inequalities,” *Phys. Rev. A*, vol. 66, no. 3, p. 032319, Sep. 2002, doi: 10.1103/PhysRevA.66.032319.
[22] K. J. Lee and C. T. Mueller, “Adapting computational protein folding logic for growth-based, assembly-driven spatial truss design,” *Proc. IASS Annu. Symp.*, vol. 2020, no. 7, pp. 1–13, Jun. 2020.
[23] V. S. Deshpande, N. A. Fleck, and M. F. Ashby, “Effective properties of the octet-truss lattice material,” *J. Mech. Phys. Solids*, vol. 49, no. 8, pp. 1747–1769, Aug. 2001, doi: 10.1016/S0022-5096(01)00010-2.
[24] X. Zheng *et al.*, “Ultralight, Ultrastiff Mechanical Metamaterials,” *Science*, vol. 344, no. 6190, pp. 1373–1377, 2014.
[25] K. Miura and S. Pellegrino, Eds., “Space Frames,” in *Forms and Concepts for Lightweight Structures*, Cambridge: Cambridge University Press, 2020, pp. 28–58. doi: 10.1017/9781139048569.003.
[26] H. Poincaré, “Analysis situs,” *Journal de l’École Polytechnique*, 1895. https://gallica.bnf.fr/ark:/12148/bpt6k4337198 (accessed Jan. 21, 2023).
[27] D. López and R. B. Fuller, *R. Buckminster Fuller: pattern-thinking*. Zurich, Switzerland: Lars Müller Publishers, 2020.
[28] J. H. Conway and N. J. A. Sloane, *Sphere Packings, Lattices and Groups*, vol. 290. in Grundlehren der mathematischen Wissenschaften, vol. 290. New York, NY: Springer New York, 1999. doi: 10.1007/978-1-4757-6568-7.
[29] E. S. Popko and C. J. Kitrick, *Divided Spheres: Geodesics and the Orderly Subdivision of the Sphere*, 2nd ed. New York: A K Peters/CRC Press, 2021. doi: 10.1201/9781003134114.
[30] R. B. Fuller, *Synergetics: explorations in the geometry of thinking*. New York: MacMillan, 1982.
[31] R. Abbott, “What Makes Complex Systems Complex?,” *J. Policy Complex Syst.*, vol. 4, no. 2, 2018, doi: 10.18278/jpcs.4.2.6.
[32] A. C. Edmondson, “Isotropic Vector Matrix,” in *A Fuller Explanation*, Boston, MA: Birkhäuser Boston, 1987, pp. 127–142. doi: 10.1007/978-1-4684-7485-5_9.
[33] T. Knight, “Computing with Emergence,” *Environ. Plan. B Plan. Des.*, vol. 30, no. 1, pp. 125–155, Feb. 2003, doi: 10.1068/b12914.
[34] T. Knight and G. Stiny, “Making grammars: From computing with shapes to computing with things,” *Des. Stud.*, vol. 41, pp. 8–28, Nov. 2015, doi: 10.1016/j.destud.2015.08.006.
[35] M. Agarwal, J. Cagan, and K. G. Constantine, “Influencing generative design through continuous evaluation: Associating costs with the coffeemaker shape grammar,” *Artif. Intell. Eng. Des. Anal. Manuf.*, vol. 13, no. 4, pp. 253–275, Sep. 1999, doi: 10.1017/S0890060499134024.
[36] H. Jones and A. Campa, “Fractals Based on Regular Polygons and Polyhedra,” in *Scientific Visualization of Physical Phenomena*, N. M. Patrikalakis, Ed., Tokyo: Springer Japan, 1991, pp. 299–314.

[37] A. W. F. Edwards, *Pascal's arithmetical triangle: the story of a mathematical idea*. Baltimore: Johns Hopkins University Press, 2002.
[38] J. Shah, "A history of Piṅgala's combinatorics," p. 44, 1991.
[39] J. H. Conway and N. J. A. Sloane, "Low–dimensional lattices. VII. Coordination sequences," *Proc. R. Soc. Lond. Ser. Math. Phys. Eng. Sci.*, vol. 453, no. 1966, pp. 2369–2389, Nov. 1997, doi: 10.1098/rspa.1997.0126.
[40] "OEIS Foundation Inc. (2023), Tetrahedral numbers, Entry A000292 in The On-Line Encyclopedia of Integer Sequences, http://oeis.org/A000292."
[41] V. S. Deshpande, M. F. Ashby, and N. A. Fleck, "Foam topology: bending versus stretching dominated architectures," *Acta Mater.*, vol. 49, no. 6, pp. 1035–1040, Apr. 2001, doi: 10.1016/S1359-6454(00)00379-7.
[42] A. K. Noor and M. M. Mikulas, "Continuum Modeling of Large Lattice Structures: Status and Projections," in *Large Space Structures: Dynamics and Control*, S. N. Atluri and A. K. Amos, Eds., in Springer Series in Computational Mechanics. Berlin, Heidelberg: Springer Berlin Heidelberg, 1988, pp. 1–34. doi: 10.1007/978-3-642-83376-2_1.
[43] J. C. Maxwell, "L. On the calculation of the equilibrium and stiffness of frames," *Lond. Edinb. Dublin Philos. Mag. J. Sci.*, vol. 27, no. 182, pp. 294–299, Apr. 1864, doi: 10.1080/14786446408643668.
[44] A. G. Bird, "Optimization of Highly Architectured Stereolithographic Microtrusses," M.A.S., University of Toronto (Canada), Canada -- Ontario, CA. Accessed: Jan. 14, 2023. [Online]. Available: https://www.proquest.com/docview/1739002471/abstract/D00EC9058594E04PQ/1
[45] T. J. Collins, "Generation and analysis of reduced-part-count truss geometries for space-based applications".
[46] H. Lalvani and T. J. Collins, "Comparative morphology of configurations with reduced part count derived from the octahedral-tetrahedral truss," NAS 1.15:102768, Feb. 1991. Accessed: Sep. 06, 2022. [Online]. Available: https://ntrs.nasa.gov/citations/19910009855
[47] T. Munzner, "Geodesic Dome Assembly." https://graphics.stanford.edu/~munzner/dome/struts/
[48] H. Wadley, "Fabrication and structural performance of periodic cellular metal sandwich structures," *Compos. Sci. Technol.*, vol. 63, no. 16, pp. 2331–2343, Dec. 2003, doi: 10.1016/S0266-3538(03)00266-5.
[49] H. Wadley, Deshpande, Vikram, and Berger, Jonathan, "Ultralight Lattice-based Materials for Multifunctional Space Structures," *NASA ESI Quad Chart*, 2017.